ELSEVIER J. Non-Newtonian Fluid Mech., 54 (1994) 153–193

Journal of Non-Newtonian Fluid Mechanics

Normal stresses in fibre suspensions ☆

M.A. Zirnsak, D.U. Hur, D.V. Boger *

Department of Chemical Engineering, The University of Melbourne, Parkville 3052, Australia

Received 26 April 1994

Abstract

Existing constitutive theories for fibre suspensions in Newtonian suspending media adequately predict the steady shear and extensional viscosity for such dilute and semi-dilute suspensions, but most do not predict the finite normal stresses observed for non-dilute fibres suspended in a Newtonian liquid. Normal stresses were measured for suspensions of rigid glass fibres in Newtonian fluids. The fibres were 3.2 mm (1/8″) and 6.4 mm (1/4″) long, having aspect ratios of 276 and 552 respectively. The first normal stress difference was found to vary approximately linearly with shear rate and its magnitude increased with increasing fibre concentration and aspect ratio. The fact that these observed normal stresses are not merely due to wall effects was confirmed by varying the gap in a parallel-plate geometry for the normal stress measurements. It was found that the normal stresses observed in steady state shear were adequately predicted by the equation derived by Carter [L.F. Carter, A Study of the Rheology of the Suspensions of Rod-Shaped Particles in a Navier–Stokes liquid, Ph.D. Dissertation, University of Michigan, Ann Arbor, MI, 1967].

Keywords: Fibre; Shear rate; Stress; Suspensions

1. Introduction

1.1. General

The reinforcement of polymeric materials with short fibres offers both mechanical and economic advantages for many applications. Hence an understanding of the

* Corresponding author.

☆ Dedicated to Professor Ken Walters FRS on the occasion of his 60th birthday.

SSDI 0377-0257(94)01323-A

rheology of fibre suspensions is currently of both practical and theoretical interest. A large number of experimental works in various flow geometries have been published for concentrated fibre suspensions. These systems are so complex that generalisations cannot be made for them. The findings of these works have often contradicted one another. Owing to the large number of variables present in fibre reinforced polymer suspensions, it has been necessary for theoretical predictions to start with the simpler case of fibres suspended in a Newtonian liquid.

This paper reviews the theories currently available for the prediction of the rheological properties of fibre suspensions. Comparison will then be made between the theories and the experimental measurements. A very good review of experimental work done on fibre suspensions up until 1985 is available [1].

Most continuum theories predict that the first normal stress differences at steady state are very small or zero for semi-dilute suspensions of rigid fibres in a Newtonian solvent. However, previous experimental work has shown that such suspensions exhibit finite normal stresses in steady state shear. Thus experimental measurements of the first normal stress differences of semi-dilute suspensions of glass fibres in a high viscosity Newtonian solvent were carried out and compared with the existing theories to see if any of the theories adequately predicted the observed normal stress behaviour at steady state.

1.2. Theoretical background

The basis for all current models for fibre suspensions is the theory of Jeffery [2] for the motion of a single ellipsoid in a Newtonian fluid. However, Brenner [3] pointed out that whether the ends of the suspended particles are "pointed" (as in the case of a prolate spheroid) or "blunt" (as in the case of a cylindrical rod) is crucial in relating rheological and analogous transport properties to the longitudinal and transverse dimensions of the long slender body.

For suspensions of non-spherical particles such as rigid rod-like macromolecules and short glass fibres, three different concentration regions — dilute, semi-dilute, and concentrated — are defined in terms of particle volume fraction, ϕ, and particle aspect ratio, r [4]. The dilute range is when

$$\phi r^2 \ll 1, \tag{1}$$

the semi-dilute range is given by

$$r^{-2} \ll \phi \ll r^{-1} \tag{2}$$

and finally the concentrated region is defined as

$$\phi r \gg 1. \tag{3}$$

Suspensions of glass fibres in a Newtonian fluid may be effectively treated as a continuum, provided that the fibre length is much less than the scale of the flow and the volume fraction of the suspended fibres is small. The effect of rotary Brownian motion is usually negligible for glass fibre suspensions from the fact that the

rotational diffusivity (D_r) is usually very small, particularly for high aspect ratio fibres in highly viscous solvents [5].

1.3. Continuum theories

With few exceptions, the available continuum theories contain the following assumptions:

(i) the volume fraction, ϕ, of the particles is extremely small so that there is no hydrodynamic interaction between fibres, or between fibre and boundary, i.e. $\phi \ll 1$ or $\phi r^2 \ll 1$;
(ii) the particle length is much less than the geometrical dimensions of the flow and the fibre aspect ratio, r, is uniform;
(iii) the effects of rotary Brownian motion, inertia, and external body forces are negligible;
(iv) the suspending medium is a uniform incompressible Newtonian fluid.

From continuum theory, the rheological properties of dilute fibre suspensions are predicted never to reach steady state, but to oscillate with time, owing to the time-dependence of the particle orientation distribution. For example, Okagawa et al. [6] predicted, for a model suspension of prolate spheroids in a Newtonian fluid, that, in the absence of particle interactions and Brownian motion, the intrinsic viscosity, $[\eta]$, and the intrinsic first normal stress difference, $[N_1]$, never reach steady state, but oscillate with a frequency twice that of a particle rotation about the vorticity axis. The intrinsic viscosity was defined as

$$[\eta] = \lim_{\phi \to 0} \frac{\eta - \eta_s}{\phi \eta_s} \tag{4}$$

and the intrinsic first normal stress difference as

$$[N_1] = \lim_{\phi \to 0} \frac{N_1}{\phi \eta_s \dot{\gamma}} \tag{5}$$

where η is the suspension viscosity, η_s is the solvent viscosity, N_1 is the suspension first normal stress difference and $\dot{\gamma}$ is the shear rate.

In experiments, the initially isotropic (random) orientation of the particles rapidly reaches steady state [5,7–21]. Anisotropy of particle orientation at equilibrium, induced by flow, or any other mechanism, will cause anisotropy in the rheological properties of dilute fibre suspensions. Such equilibrium orientation distribution can be obtained in a few particle rotations even for very dilute suspensions. For real fibre suspensions, particle interactions (which are believed to involve hydrodynamic rather than mechanical contact for semi-dilute suspensions [22]), polydispersity of particle aspect ratio and non-uniform shear rate appear to be the major factors in bringing about the rapid approach to steady state.

Although a number of experimental observations for model fibre suspensions are available, the range of fibre volume concentrations investigated is often too high for the continuum theory to be applicable. From experimental results [23,24] it can be suggested that fibre–fibre and fibre–boundary interactions are the major parame-

ters in determining the rheological properties of non-dilute fibre suspensions at steady state.

Okagawa and Mason [24] indirectly determined the rheological properties of a dilute particle suspension ($\phi r^2 = 0.29$) of nylon fibres in a silicone oil from the measured orientation distributions, and made a comparison with predicted values. The intrinsic first normal stress difference, $[N_1]$, was predicted to continue damped oscillations of frequency $2/T^*$, where T^* is the period of one particle rotation, until $[N_1]$ reaches zero, independent of shear rate, $\dot{\gamma}$. The values computed from measured orientations were in good agreement with predictions, but started to deviate around $t = T^*$, where t is the time from start-up, because of irreversible particle interactions.

Batchelor [25] developed a general constitutive equation for the bulk stress in a suspension of force-free particles of any shape at arbitrary concentration in a Newtonian liquid. Batchelor also applied this general result to the specific problem of non-dilute suspensions of long "slender" bodies subjected to a simple extensional flow [26]. In this case, "non-dilute" means that the volume fraction of fibres and the fibre aspect ratio are in the range of values such that the average distance between the fibres is greater than the fibre radius, but less than half the fibre length. It should be noted that Batchelor's theory predicts a constant extensional viscosity which is large compared to the extensional viscosity of the Newtonian suspending fluid.

Dinh and Armstrong [27] developed a constitutive equation for semi-dilute fibre suspensions in Newtonian fluids. In their equation, Batchelor's theory is used to modify the force exerted on the fibre by the suspending liquid in such a way as to try and take into account the presence of other particles. It was predicted that the transient shear viscosity, η^+, defined by the ratio of time-dependent shear stress to constant shear rate, $\dot{\gamma}$, is a constant at fixed strains, and at steady-state ($\gamma = \dot{\gamma}t \to \infty$, where γ is the total strain), $\eta^+ \to \eta$ (steady shear viscosity), whereas the transient normal stress differences vary with $\dot{\gamma}^2$, but vanish at steady state. The predictions are essentially the same as those predicted by the continuum theory for dilute fibre suspensions. In steady shear flow the fibres align with the flow and their effect, according to the approximation used, vanishes. The thickness of the fibre is neglected as far as hydrodynamic interactions are concerned, and so in simple shear a fibre aligned with the direction of flow feels no force, and therefore remains aligned in this direction and does not affect the flow.

In shear viscosity measurements the induced particle orientation results in the particle diameter becoming the most important dimension to be considered. Hence, wall effects will usually be small as the characteristic dimensions of the measuring apparatus are usually much larger than the particle diameter [28]. However, with experiments involving randomly oriented fibre suspensions, where fibre length is the most important particle dimension, it is almost impossible to neglect wall effects [29] because the characteristic dimensions of the measuring apparatus are then comparable with those of the fibres. The wall effects of semi-dilute randomly oriented fibre suspensions in the shear flow between two parallel plates were investigated theoretically and experimentally by Bibbo et al. [23]. Using gaps which

are approximately the same size as the particle length results in measurements which do not truly reflect the material properties of randomly oriented suspensions.

1.4. Theoretical predictions for the viscosity of fibre suspensions

A suspension of uniform fibres has a viscosity which depends upon the detailed geometrical description of the fibres, their orientation distribution, as well as the volume fraction of fibres. A number of expressions for the viscosity of fibre suspensions are available in the literature; for completeness we list them all.

Jeffery [2] wished to determine the viscosity increase of a suspension over its solvent due to the presence of hydrodynamically isolated non-spherical particles. However, the rotations of the particles rendered his energy dissipation calculation indeterminate, owing to the effect of instantaneous particle orientation and the need to know the initial particle orientation.

Guth [30] derived a theoretical expression for the viscosity of a dilute suspension of rigid elongated ellipsoids for the case of maximum energy dissipation. The result obtained was

$$\eta_r = 1 + ([p/2(\ln 2p - 1.5)] + 2)\phi, \tag{6}$$

where η_r is the relative viscosity given by $\eta_r = \eta/\eta_s$, p is the axial ratio of the ellipsoids.

Burgers' [5] work indicates that the predicted viscosities for rigid elongated ellipsoids and rods are essentially the same if the constant 1.5 in Eq. (6) is replaced by 1.8. By using the Eisenshitz [31,32] assumption, Burgers derived, for suspensions of dilute thin rigid rods, the relation

$$\eta_r = 1 + [2r\phi/3\pi(\ln 2r - 1.8)]. \tag{7}$$

Simha [33] derived an expression for the steady-shear viscosity of dilute suspensions of rigid rods, where $r > 10$, in the limit of zero shear rate, and where Brownian motion is important. The expression obtained was

$$\eta_r = 1 + \phi\left[\frac{r^2}{15(\ln 2r - 1.8)} + \frac{r^2}{5(\ln 2r - 0.8)} + \frac{14}{15}\right]. \tag{8}$$

Kuhn and Kuhn [34] derived expressions for the viscosity of dilute suspensions of rigid ellipsoids for which Brownian motion was dominant. For $1 < p < 15$,

$$\eta_r = 1 + 2.5\phi + 0.4075(p - 1)^{1.508}\phi \tag{9}$$

and for $p > 15$,

$$\eta_r = 1 + 1.6\phi + \frac{p^2}{5}\left[\frac{1}{3(\ln 2p - 1.5)} + \frac{1}{\ln 2p - 0.5}\right]\phi. \tag{10}$$

Scheraga [35] calculated the viscosity of suspensions of prolate and oblate ellipsoids, and presented his results in the form of tables and graphs of intrinsic viscosity with changing Péclet number and aspect ratio. At zero Péclet number he obtained the same equation as Simha [33] for prolate ellipsoids.

Nawab and Mason [36] suggested that an equivalent ellipsoidal aspect ratio, r_e, be used in the results obtained from Jeffery's equations by Burgers. Using this modification the expression for the relative viscosity becomes

$$\eta_r = 1 + 2r^2\phi/3\pi r_e(\ln 2r - 1.8). \tag{11}$$

Brodnyan [37] derived a semi-empirical expression for the viscosity of suspensions of rigid ellipsoids in which only interactions due to crowding, i.e. first-order interactions, were considered. The result was

$$\eta_r = \exp\left[\frac{2.5\phi + 0.399(p-1)^{1.48}\phi}{1 - K_1\phi}\right], \tag{12}$$

where K_1 is an interaction constant. When $p = 1$, $K_1 = 1.35$; however as p increases, then K_1 rapidly and asymptotically approaches 1.91. There was no restrictions on the concentration range over which the equation was valid.

Blakeney [38] gave a general experimental viscosity–concentration relationship for suspensions as

$$\eta_r = 1 + K_2\phi + K_3\phi^2, \tag{13}$$

where K_2 is a dimensionless factor determined by the shape, dimensions, and orientations of the suspended particles, and the $K_3\phi^2$ term accounts for particle interactions, both hydrodynamic and mechanical. The interaction term can also be written $K_4(K_2\phi)^2$, where it has been found that $K_4 = 0.73$ for purely hydrodynamic interactions between rigid rods, randomly orientated by Brownian motion. This term is only considered when $\phi > \phi_0$, where $\phi_0 = 1.5r^2$, which is the "critical concentration" for free rotation of the fibres. The theory of Burgers [5] was used to give

$$K_2 = \frac{2r}{3\pi(\ln 2r - 1.8)}. \tag{14}$$

Ziegel [39] derived the following equation for the viscosity of suspensions of elongated rods in high-viscosity fluids:

$$\eta_r = 1 + (1 - z + (3\mu z\chi/\dot{\gamma}))(r^{5/3}\phi/9.668) \tag{15}$$

where χ is a rate constant for the equilibrium between free particles and agglomerates, μ is a closeness of approach factor which is like a coefficient of friction, and z is a factor giving the degree of agglomeration. The equation predicts that the suspension will be shear thinning.

Leal and Hinch [40] predicted that the relative viscosity of a very dilute suspension of spheroids with axis ratio p, in the case where Brownian diffusion is small but dominant over the effects of inertia and particle–particle interactions, in the limit of infinite p is

$$\eta_r = 1 + \left(2 + \frac{0.312p}{\ln 2p - 1.5}\right)\phi. \tag{16}$$

The result is valid when $1 \ll Pe \ll p^3$, where the Péclet number is given by $Pe = \dot{\gamma}/D_r$ and D_r is the rotary diffusion coefficient. It was stated that this result could be applied to any body of revolution, except certain very long particles, by the substitution of an effective aspect ratio, r_e, for the particle in question for p. The value of r_e depends on the precise shape of the particle.

Hinch and Leal [13] predicted the relative viscosity for dilute suspensions of ellipsoids, finding the expression was dependent on the Péclet number. For weak Brownian motion, when $p^3 \ll Pe$, and in the case where $p \to \infty$, then

$$\eta_r = 1 + (0.315p\phi/\ln p). \tag{17}$$

When $1 \ll Pe \ll p^3$, intermediate Brownian motion, and $p \to \infty$, then

$$\eta_r = 1 + (0.5p^2\phi/Pe^{1/3} \ln p). \tag{18}$$

Finally, for dominant Brownian motion, where $Pe \ll 1$, and in the case where $p \to \infty$,

$$\eta_r = 1 + (4p^2\phi/15 \ln p). \tag{19}$$

Hinch and Leal [14] computed that dilute suspensions of ellipsoidal particles that are rod-like will show shear-thinning behaviour. At zero shear rate the suspension will have a viscosity of η_0, while at high shear rates the shear viscosity reaches a constant value of η_∞, given by

$$\eta_\infty/\eta_0 = 1.181/p. \tag{20}$$

Brenner [3] provides very comprehensive results for the viscosity of dilute suspensions of axisymmetric rigid particles in Newtonian solvents. It is demonstrated that the rheological properties can be expressed in terms of five fundamental, non-dimensional material constants (exclusive of solvent viscosity), which depend only on the sizes and shapes of the suspended particles. It was discovered that circular cylindrical rods are not adequately modelled by long thin prolate spheroids. Separate expressions are given for the viscosity of dilute suspensions of rigid particles for the cases of dominant Brownian motion, intermediate Brownian motion and weak Brownian motion. Brenner obtains the same result as Simha [33] and Scheraga [35] for the zero-shear relative viscosity of suspensions of long thin prolate ellipsoids. Also for ellipsoids, where $p \gg 1$ and Brownian motion is dominant, Brenner obtains the same equation as Kuhn and Kuhn [34]. Only the results for long cylindrical fibres, where $r \gg 1$, will be presented here. Dominant Brownian motion is defined by $BPe \ll 1$, where B is given by

$$B = 1 - \frac{3K_5 \ln r}{4\pi r^2}. \tag{21}$$

K_5 is a numerical constant having a value of around 5.45 for circular cylinders of finite length, and Pe is the Péclet number, $Pe = \dot{\gamma}/D_r$. The rotary diffusion coefficient, D_r, is given by

$$D_r = kT/6V_p\eta_s{}'K_\perp, \tag{22}$$

where V_p is the volume of a particle, k is Boltzmann's constant, T is the absolute temperature, and ${}^{r}K_{\perp}$ for cylindrical fibres with $r \gg 1$ is given by

$$ {}^{r}K_{\perp} = \frac{2}{9}\left[\frac{r^2}{\ln r}\left(1 - \frac{1 - \ln 2}{\ln r}\right) + \frac{3K_5}{8\pi}\right]. \tag{23} $$

Brenner's calculations can be used to derive the following expressions for the relative viscosity. In the limiting case where $BPe = 0$,

$$ \eta_r = 1 + (2 - Q_2 + 2Q_3)\phi \tag{24} $$

where

$$ Q_2 = \frac{-2r^2}{45[\ln 2r + \ln 2 - (17/6)]} \tag{25} $$

$$ Q_3 = (B/15)\left[\frac{r^2}{\ln r}\left(1 - \frac{1 - \ln 2}{\ln r}\right) - \frac{3K_5}{8\pi}\right]. \tag{26} $$

For $BPe \ll 1$, correct to terms of $O([BPe]^2)$,

$$ \eta_r = 1 + \left[2 - Q_2 + 2Q_3 - \frac{(BPe)^2}{1260}(12Q_2 + 6Q_3 + 35N/B)\right]\phi \tag{27} $$

where

$$ N = \frac{2}{15}\left[\frac{r^2}{\ln r}\left(1 - \frac{1 - \ln 2}{\ln r}\right) - \frac{3K_5}{8\pi}\right]. \tag{28} $$

In the intermediate case, where $r_e \gg Pe^{-1/3} \gg 1$ and where r_e is the equivalent aspect ratio of the fibres, given by

$$ r_e = (8\pi r^2/3K_5 \ln r)^{1/2}, \tag{29} $$

the relative viscosity becomes

$$ \eta_r = 1 + [2 + (15/4)(B^{-1} - 1)Q_2 - KPe^{-1/3}]\phi \tag{30} $$

where

$$ K = 0.822Q_2 + 5.388(B^{-1} - 1)Q_2. \tag{31} $$

Finally, for weak Brownian motion, where $Pe^{1/3} \gg r_e \gg 1$, the relative viscosity becomes

$$ \eta_r = 1 + \left\{2 - (15/4)\left[Q_1\left(1 - \frac{1.792}{r_e}\right) - (Q_2/B)\left(1 - \frac{3.0524}{r_e}\right) - (r_e^2/BPe^2)(3Q_2 + 4Q_3)\right]\right\}\phi. \tag{32} $$

Fedors [41,42] presented the following equation for the viscosity of suspensions:

$$ \eta_r = \left(1 + \frac{1.25\phi}{\phi_m - \phi}\right)^2 \tag{33} $$

where ϕ_m is the maximum volume fraction to which the particles can pack. No theoretical derivation, limit to the concentration range over which the equation is applicable, or shapes of particles that the equation applies to were given by Fedors. Hence its applicability to suspensions of rigid rods may be considered dubious.

Maschmeyer and Hill [43] state that a theory developed by Nielsen [44] for elastic moduli can be used to predict the viscosity of suspensions of rods. The equation is

$$\eta_r = \frac{1 + (K_6 - 1)C\phi}{1 - C\psi\phi}, \tag{34}$$

where

$$\psi = 1 + \frac{(1 - \phi_m)}{\phi_m^2}\,\phi, \tag{35}$$

$$K_6 = \lim_{\phi \to 0} \eta_r - 1 \tag{36}$$

and C is very nearly unity for rigid particles in a viscous medium. ϕ_m is the maximum possible volume fraction. As these equations were not actually derived for fibre suspensions their use for such may be considered dubious.

The theory of dilute solution of rod-like macromolecules, which can also be applied to macroscopic fibres, suggests [45,46]

$$\eta \approx \eta_s + ckT/D_{ro}, \tag{37}$$

where c is the number of rods per unit volume, and D_{ro} is a rotational diffusion constant in dilute solution, given by

$$D_{ro} = kT \ln r/3\pi\eta_s L^3 \tag{38}$$

where L is the length of the rod. Thus for dilute suspensions

$$\eta_r \approx 1 + cL^3. \tag{39}$$

Since the equation is correct for the dilute solution region, i.e. $c \ll 1/L^3$, the viscosity due to rods is always small compared with the solvent viscosity in dilute solution.

Doi and Edwards [47] gave the following equation for semi-dilute suspensions of rigid rods:

$$\eta_r = 1 + (cL^3)^3. \tag{40}$$

Since the suspension is in the concentration region $cL^3 \gg 1$, the viscosity, η, is much greater than the solvent viscosity, η_s. Further, since this very large viscosity is due to the rods which have rotational degrees of freedom, the viscosity is very sensitive to the magnitude of the shear rate and shear history. Such shear-rate and shear-history dependence of viscosity also occur in dilute solution, but there it is always only a small correction to the solvent viscosity. In concentrated solution most of the viscosity is due to the rods which are sensitive to external forces. Further, Doi and Edwards [47] predicted that semi-dilute suspensions of rods would have constant

viscosity up to Péclet numbers of around unity and thereafter show shear-thinning behaviour. The zero-shear viscosity was given by

$$\eta_0 = ckT/10D_r. \tag{41}$$

The approximation of the average rotational diffusivity, D_r, is given by

$$D_r = \beta D_{ro}/(cL^3)^2, \tag{42}$$

where D_{ro} is given by Eq. (38) and β is a numerical factor. Doi and Edwards [47] state that β is in the order of unity; however, in their later book it is stated that various data suggest that β is rather large, in the order of 10^3 [48], while Milliken et al. [49] found $\beta \approx 70$ from experimental measurements of the viscosity of isotropic suspensions using falling ball rheometry.

Haber and Brenner [50] derived the steady-state rheological properties of a dilute monodisperse suspension of centrosymmetric particles subject to a general isochoric shearing flow where Brownian motion is dominant. They found that Simha's [33] derivation is conceptually incorrect, but gives the correct result for the zero-shear viscosity of dilute Brownian spheroid suspensions.

Bibbo et al. [23] predicted that for semi-dilute suspensions of rigid fibres

$$\eta_r = \frac{1}{1-(4\phi/\pi)^{1/2}}. \tag{43}$$

It was also found that the dependence of η on shear rate is of the same form as for η_s. The suspension viscosity as a function of shear rate is simply obtained by shifting the η_s curve to lower shear rates by a factor of $[1-(4\phi/\pi)^{1/2}]^{-1}$ and by increasing its magnitude by the same factor. This means that if the solvent is shear thinning, the suspension will show the shear-thinning behaviour at lower shear rates than the solvent.

Berry and Russel [51] derived an expression for the relative viscosity of dilute suspensions of slender rods where $Pe \ll 1$, $r \gg 1$ and $(\ln 2r)^{-1} \ll 1$, and where interactions between particles are weak and long range. The equations given, up to $O(\phi^2)$, are

$$\eta_r = 1 + [\eta]\phi + K_7[\eta]^2\phi^2 \tag{44}$$

with

$$[\eta] = \frac{8r^2}{45 \ln 2r}(1 - 0.020Pe^2) \tag{45}$$

$$K_7 = (2/5)(1 - 0.0142Pe^2). \tag{46}$$

Table 1 provides a summary of the applicability of all the theories for the relative viscosity of suspensions of rods and ellipsoids reviewed, and whether or not these theories predict shear-thinning behaviour for the suspensions.

It should also be noted that, for suspensions of large aspect ratio fibres ($r > 10$), two critical concentrations are present: the first occurs when $\phi = 3/2r^2$, beyond which the fibres can no longer rotate freely without interparticle interactions so that

Table 1
Summary of the theories for the relative viscosity of dilute and semi-dilute suspensions of rigid ellipsoids and rods

Reference	Applicable concentration	Shape of particles	Applicable *Pe*	Predicts shear tinning
Guth (1938) [30]	Dilute	Ellipsoids	$Pe \to \infty$	No
Burgers (1938) [5]	Dilute	Rods	$Pe \to \infty$	No
Simha (1940) [33]	Dilute	Ellipsoids Rods ($r > 10$)	0	No
Kuhn and Kuhn (1945) [34]	Dilute	Ellipsoids	0	No
Scheraga (1955) [35]	Dilute	Ellipsoids	$0 \leqslant Pe \leqslant 60$	Yes
Nawab and Mason (1958) [36]	Dilute	Ellipsoids and rods	$Pe \to \infty$	No
Brodnyan (1959) [37]	All	Ellipsoids	All	No
Blakeney (1966) [38]	Dilute and semi-dilute	Rods	All	No
Nielsen (1970) [44]	All	Any	All	No
Ziegel (1970) [39]	All	Rods	All	Yes
Yamakawa (1971) [46]	Dilute	Rods	All	No
Leal and Hinch (1971) [40]	Dilute	Ellipsoids	$1 \ll Pe \ll p^3$	No
Hinch and Leal (1972) [13]	Dilute	Ellipsoids ($p \to \infty$)	All	Yes for $1 \ll Pe \ll p^3$
Brenner (1974) [3]	Dilute	Ellipsoids and rods	All	Yes for $Pe \gg 1$
Fedors (1974) [41]	All	Any	All	No
Bird et al. (1977) [45]	Dilute	Rods	All	No
Doi and Edwards (1978) [47]	Semi-dilute	Rods	All	Yes
Bibbo et al. (1985) [23]	Semi-dilute	Rods	All	No
Berry and Russel (1987) [51]	Dilute	Rods ($r \gg 1$)	$Pe \ll 1$	Yes

the fibre interactions cause a significant increase in the viscosity [52]. The second regime is estimated on the assumption that every fibre has at least three contact points with other adjacent fibres and occurs when $\phi \approx 108\pi/r^2$, above which the fibres may form transient network structures [53]. The average size of these transient fibre aggregates depends upon the rate of deformation, fibre concentration, and aspect ratio, implying that non-dilute fibre suspensions in the second regime may be shear thinning.

1.5. Experimental measurements of the viscosity of fibre suspensions

A large number of workers have reported that the viscosity of fibre suspensions increases with increasing volume fraction of fibres [11,23,36,38,39,43,49,54–65], and

with increasing aspect ratio [58–61]. Blakeney [38] and Goto et al. [59] also found that increasing the fibre flexibility increases the relative viscosity of the suspension. Discrepancy occurs, however, between those workers who observed shear thinning in their fibre suspensions [36,39,43,54,55,57–59,61,65] and those who did not [23,49,56,60,64,66–68]. Shear thinning appeared to be observed more in suspensions of higher concentration and those with large aspect ratio fibres. In their review, Ganani and Powell [1] found that as fibre aspect ratio increased, stronger shear thinning was observed with a slight dependency upon fibre concentration. The shear-thinning suspensions quite often show regions of Newtonian behaviour at both low and high shear rates, only exhibiting shear-thinning behaviour in between the two Newtonian regions [1].

The shear-thinning behaviour of non-dilute fibre suspensions may be explained by the destruction of transient network structures of fibres at higher shear rates, or anisotropic fibre orientation in the flow direction. Faitel'son and Kovtun [57] found that at a certain threshold concentration of fibres in a viscous matrix a continuous mesh is formed and, as a result, the maximum viscosity of the suspension increases. Ganani and Powell [60] found that for narrowly distributed particles, increasing the aspect ratio increases the dependency of relative viscosity, η_r, upon ϕ. It was also felt that the possibility existed that many of the measurements which showed strong shear-thinning effects in fibre suspensions did not accurately reflect the true macroscopic rheological behaviour of the suspensions and that measuring artefacts may have been present.

Maschmeyer and Hill [43,62] explained the strong dependence of the viscosity on the shear rate by a mechanism in which the actual shear rate exerted on the suspending fluid is higher than the apparent shear rate due to the presence of the suspended particles; this causes a reduction in the non-Newtonian viscosity of the suspending fluid, which in the absence of fibres is Newtonian over the range of accessible shear rates. The effect was more pronounced at higher shear rates and fibre concentrations. The same explanation was also used by Charrier and Rieger [69].

Comparing the results of Milliken et al. [49] with those of Mondy et al. [64], it was found that the viscosity of randomly oriented fibre suspensions was higher than that of aligned fibre suspensions for the same fibre aspect ratio and volume fraction. In both cases, falling ball rheometry was used so that the initial fibre orientation distribution is disturbed as little as possible, which it is not possible to do with conventional rheometers.

1.6. Observations of storage modulus for glass fibre suspensions

Ganani and Powell [60] found for suspensions of glass fibres, with mean aspect ratios of 24.3 and 7.63, in a Newtonian suspending liquid that oscillatory shearing tests showed no elastic effects, i.e. no significant storage modulus, G', and, for small strains, showed no strain dependence. This supports the result from Dinh and Armstrong's model [27].

Carter [54] found that for semi-dilute glass fibre suspensions, the phase lag observed in oscillatory flow did not increase for the suspension over the phase lag observed for the solvent.

1.7. Theoretical predictions for the extensional viscosity of non-dilute fibre suspensions

Batchelor's [26] expression for the extensional viscosity of a non-dilute fibre suspension is

$$\eta_e = 3\eta_s[1 + 4\phi r^2/9 \ln(\pi/\phi)], \tag{47}$$

where η_s is the steady shear viscosity of the suspending medium and η_e is the extensional viscosity. Very high values of the ratio η_e/η_s may be predicted within the range of validity of this theory. The equation is valid only in the range $D \ll 2h \ll L$, where D is the fibre diameter, and h is the average spacing between a fibre and its nearest neighbour and is equal to $(4\phi/\pi D^2)^{-1/2}$. The equation does not reduce to the dilute suspension theory at lower concentrations; however, the two theories predict an identical result at an intermediate concentration level.

Brenner [3] predicts the extensional viscosity for uniaxial extensional flow for dilute suspensions of rigid axisymmetric particles. In the limit of zero elongational rate, for dilute suspensions of cylinders where $r \gg 1$, the following result can be obtained from Brenner's formulae:

$$\eta_e = \eta_s(3 + [2 - Q_2 + 2Q_3]\phi) \tag{48}$$

where Q_2 and Q_3 are given by Eqs. (25) and (26). In the limit $BPe \to \infty$, where B is given by Eq. (21),

$$\eta_e = \eta_s(3 + [2 - 5Q_2]\phi). \tag{49}$$

Both Dinh and Armstrong [27] and Malamataris and Papanastasiou [70] predicted a transient extensional viscosity η_e^+ that is a function of the Hencky strain, ϵ, alone and not the extensional rate, $\dot{\epsilon}$, and time separately. The steady state value of the transient extensional viscosity for uniaxial extension was given as

$$\lim_{\epsilon \to \infty} \frac{\eta_e^+}{\eta_s} = \frac{\pi}{6}, \tag{50}$$

and at vanishing Hencky strain the limiting value was

$$\frac{\ln(2h/D)}{cL^3}((\eta_e^+/\eta_s) - 3) = \frac{\pi}{30} \tag{51}$$

where $h = (cL)^{-1/2}$ for aligned and $h = (cL)^{-1}$ for randomly oriented fibres.

Acrivos and Shaqfeh [71] predicted the extensional viscosity for non-dilute suspensions of rigid particles where $r \gg 1$, obtaining a very similar result to that of Batchelor [26]:

$$\eta_e = 3\eta_s[1 + 4\phi r^2/9 \ln(6/\phi)]. \tag{52}$$

However, their derivation used a different physical argument to Batchelor's and did not employ a "cell" model.

Shaqfeh and Fredricksen [72] found that for semi-dilute suspensions of aligned cylindrical fibres, ignoring Brownian motion, and considering only the hydro-

dynamic stress,

$$\eta_e = \eta_s \left\{ 3 + \frac{4\phi r^2}{3[\ln(1/\phi) + \ln \ln(1/\phi) + 0.1585]} \right\}. \tag{53}$$

The expression is correct to $O[1/\ln^2(1/\phi)]$. The paper was also critical of the Dinh and Armstrong [27] theories, stating that these authors have used an inappropriate average distance of closest approach between a fibre and its neighbours in their derivation, and have completely ignored interactions between particles.

Keiller et al. [73] gave the following expression for the extensional viscosity of a semi-dilute suspension of identical non-Brownian rigid rods in a Newtonian fluid:

$$\eta_e = \left(3 + \frac{K_8 \phi r^2}{\ln r} \right) \eta_s \tag{54}$$

where K_8 is a constant.

1.8. Experimental observations of the extensional viscosity of fibre suspensions

Mewis and Metzner [74] found a large, constant extensional viscosity for suspensions of glass fibres (with $r = 282$, 586, and 1259) in Indopol. The experimental data showed extensional viscosites which are independent of strain rate and as much as 260 times greater than that of the suspending fluid.

Weinberger and Goddard [68] found for suspensions of fibre-glass ($r = 57$ and $\phi = 1.3$ v/v%) in a high viscosity silicone oil and in Indopol, that the extensional viscosity was large and constant and was 26 and 23 times larger than the steady shear viscosity of the suspensions respectively. It was found that the constant viscosity was reached shortly after the suspension existed the nozzle. This indicated that extensional motion causes quick alignment of the fibres. Additional extensional strain did not appear to further align the particles, since the apparent extensional viscosity remained constant with increasing strain.

Kizior and Seyer [75] studied suspensions of rayon fibres (1.27–5.08 mm length, $r = 85$–340, and $\phi = 0.09$–0.278 v/v%) in aqueous sucrose solutions. Extensional flow was studied using an orifice and their results agreed to within 20% using Batchelor's equation [26], being slightly higher than the predicted shear stress. However, their data lend quantitative support to the dependence of bulk elongational stresses on fibre aspect ratio and concentration predicted by Batchelor.

Pittman and Byram [76] measured the extensional viscosity for 'polydisperse' carbon fibre suspensions in aqueous solutions of D-glucose. The concentration of fibres varied between 0.04 and 0.09 v/v%, while the aspect ratio varied between 50 and 300 (with the length varying between 0.5 and 3.0 mm). It was found that by using the average aspect ratio in Batchelor's semi-dilute equation [26] the predicted results closely matched the experimental results. However, when Batchelor's equation was adjusted to take into account the 'polydispersity' in the fibres, the predicted results were about 15% higher than the experimental results. Further, it was realised that the suspensions used were not strictly dilute nor semi-dilute, but somewhere in between the two regimes. Thus an interpolation equation, suggested

by Batchelor [26] for suspensions between dilute and semi-dilute ranges and adjusted to take into account 'polydispersity', was also used, but gave results that were approximately double the experimental values. It was stated that their experimental results may be on the low side owing to incomplete fibre dispersion.

Jeffrey and Acrivos [77] presented a graphical comparison between the theory of Batchelor [26] and the experimental data obtained by Kizior and Seyer [75], Mewis and Metzner [74], and Weinberger and Goddard [68]. The agreement is satisfactory and becomes better for particles having higher aspect ratios, to which the theory is more applicable.

Powell [28] compared the experimental data of Mewis and Metzner [74] and Pittman and Byram [76] with the theories of Batchelor [26], Acrivos and Shaqfeh [71], and Shaqfeh and Fredricksen [72]. It was found that all three theories fitted the data reasonably well, with the theory of Shaqfeh and Fredricksen [72] providing the best fit for the data of Pittman and Byram [76].

1.9. Weissenberg effect for fibre suspensions

According to the theory of Weissenberg, elastic elements are required in a system for it to exhibit the rod climbing (Weissenberg) effect. Usually, for polymer systems the observation of the Weissenberg effect is attributed to the presence of normal forces. Nawab and Mason [36], Mewis and Metzner [74], Roberts and Hill [78], and Han [79], observed the Weissenberg effect for fibre supsensions in a Newtonian fluid. Mewis and Metzner [74] found that rigid glass fibre suspensions ($r = 282-1259$, $D = 11$ μm, $\phi = 0.1-1\%$) in low molecular weight polybutene exhibited the Weissenberg effect, the magnitude of which increased with fibre concentration and aspect ratio. Nawab and Mason [36] observed the Weissenberg effect for suspensions of rayon fibres in castor oil only for $r \geqslant 173$. Roberts and Hill [78] observed the Weissenberg effect for suspensions of rigid glass fibres in an inelastic oil. Han [79] observed the Weissenberg effect for glass fibres ($r = 962$) in Indopol L100.

Chan et al. [80] explained the Weissenberg effect observed in fibre suspensions as follows. The shear flow of the medium between the glass fibres induces tensile stresses, and the fibre tensile stress acting along streamlines that close upon themselves results in a normal stress in the suspension which induces the Weissenberg effect.

1.10. Theoretical predictions of first normal stress difference for dilute and semi-dilute fibre suspensions

Predictions for normal stress differences in simple shear are, generally, that they are small or zero, except for those that occur during the start-up period when there are oscillating stresses arising from the tumbling motion of the particles and the fact that the particle orientation distribution has not reached steady state.

Hinch and Leal [14] considered a dilute suspension of rigid axisymmetric particles in circumstances where the shear flow alignment of the particles dominates small but not unimportant Brownian disorientation. It was stated that normal stress differences at steady state are $O(D_r)$, where D_r is the rotational diffusivity and

$D_r \ll 1$. However, they go on to state at steady state the normal stresses are $O(D_r r^3)$ smaller than the steady shear stress. Calculations for ellipsoids with an aspect ratio of only 5 give a first normal stress difference which is never more than one-third of the shear stress (due to the particles) and a second normal stress difference which is negative and less than one-tenth of the magnitude of the first [15]. The dependence of normal stresses on shear rate is initially quadratic starting from zero, as for a second-order fluid. The normal stresses tend towards a limiting value at high shear rates.

Lipscomb and co-workers [81,82] claimed that the undamped oscillation of N_1 hardly reaches a steady state for dilute fibre suspensions until the dimensionless time of shear, $t^* = \dot{\gamma} t/r$, is in order of approximately 1.0 for large aspect ratio fibres ($r > 10$).

The transient theory for semi-dilute fibre suspensions [27,70,83] predicts finite normal stresses which vary with $\dot{\gamma}^2$ during the inception of steady flow, but which completely disappear at steady state. Altan et al. [83] present predictions that the first normal stress difference will only reach zero at infinite strain.

Hinch and Leal [13] provided expressions for the first normal stress difference of dilute suspensions of ellipsoids for dominant Brownian motion, intermediate levels of Brownian motion and weak Brownian motion. For macroscopic suspensions of fibres, D_r, from Eq. (22), is very small compared to the shear rates at which normal forces are observed. Thus the condition $Pe^{1/3} \gg p \gg 1$ is always satisfied, and only the case where Brownian motion is weak needs to be considered. In this case, and when $p \to \infty$, then

$$N_1 = \phi \eta_s D_r p^4 / 4 \ln p. \tag{55}$$

For semi-dilute suspensions of rods, Doi and Edwards [47] predicted that at steady state the first and second normal stress coefficients remain constant up to shear rates of the order of D_r, and then decrease with shear rate. The zero shear value of the first normal stress difference coefficient, $\Psi_1(0)$, is given by

$$\Psi_1(0) = ckT/30D_r^2. \tag{56}$$

Beyond shear rates in the order of D_r the first normal stress coefficient decreases, and above shear rates in the order $10D_r$ the coefficient decreases with an exponent of around -1.748 with shear rate. Thus Doi and Edwards [47] predict that at extremely small shear rates, below the order of D_r, N_1 will increase with the square of the shear rate, but N_1 will increase approximately with $\dot{\gamma}^{0.252}$ above shear rates in the order of $10D_r$. The Doi–Edwards theory also predicts that N_1 increases linearly with the concentration of rods.

Brenner [3] predicted the first normal stress difference for dilute suspensions of axisymmetric rigid particles. Expressions were provided for dominant Brownian motion, intermediate levels of Brownian motion and weak Brownian motion. As the condition $Pe^{1/3} \gg r_e \gg 1$ is always satisfied for suspensions of macroscopic fibres at shear rates where first normal stress differences can be observed then, as with Hinch and Leal [13], only the case where Brownian motion is weak needs to be

considered. In the case of cylindrical fibres where $r \gg 1$, Brenner's formulae can be used to derive

$$N_1 = \frac{5\phi kT}{2V_p {}^rK_\perp}\left[B^{-1}\left(1-\frac{4.2142}{r_e}\right)(3Q_2+4Q_3)-\frac{Q_2 r^2}{8}(B^{-1}+1)\right], \tag{57}$$

where B, ${}^rK_\perp$, Q_2, and Q_3 are given by Eqs. (21), (23), (25) and (26) respectively. As B, ${}^rK_\perp$, Q_2 and Q_3 are all functions of r only, the above equation predicts that N_1 is independent of shear rate and solvent viscosity.

Mackay [84] derived expressions for the first normal stress difference of dilute fibre suspensions from Brenner's [3] work. In the case where Brownian motion is weak, the first normal stress difference is predicted to remain constant with shear rate and can be expressed as

$$N_1 = \frac{\phi D_r \zeta_r}{8V_p}\{(1/6)r_e^2 - 2 + (6.048/r_e)\} \tag{58}$$

where

$$\zeta_r = \frac{\pi\eta_s L^3}{3\ \ln(\xi_H/D)} \tag{59}$$

and the screening length, ξ_H,

$$\xi_H = (V_p/\phi D^2 L)^{1/2}. \tag{60}$$

Given that for a cylindrical particle

$$V_p = \pi D^2 L/4 \tag{61}$$

then for cylindrical fibres,

$$\xi_H = (\pi/4\phi)^{1/2}. \tag{62}$$

D_r and r_e are given by Eqs. (22) and (29) respectively.

Mackay [84] has also predicted, using the results of Happel and Brenner [85], that N_1 for a dilute fibre suspension flowing between two parallel plates will be of the form

$$N_1 = K_9 \phi \eta_s \dot{\gamma} \Delta^2 / L^2, \tag{63}$$

where K_9 is a constant and Δ is the distance between the plates.

Carter [54] and Carter and Goddard [55] claimed, which is not obvious, that Ericksen's continuum model [86] predicts a linear dependence of the normal stresses on shear rate. Stover et al. [22], using Batchelor's theory [26], also predicted that the first normal stress difference would be proportional to the shear rate.

Carter [54] found that 'truly' dilute suspensions of elongated particles will not exhibit steady non-zero normal stresses for simple shear flow. However, for non-dilute fibre suspensions in Newtonian fluids where the fibres are of large aspect ratio the following equation was presented that predicted the first normal stress

difference:

$$N_1 = K_{10}\eta_s\dot{\gamma}\,\frac{\phi r^{3/2}}{\ln 2r - 1.8} \tag{64}$$

where K_{10} is a constant. Eq. (64) was derived on the basis of Jeffery's maximum energy dissipation [2] as well as on the assumption that collisions between the fibres are the major cause for non-zero normal stresses in steady shear flow.

1.11. *Experimental observations of first normal stress difference in fibre suspensions*

A number of workers have observed non-zero first normal stress differences in steady shear for non-dilute fibre suspensions in Newtonian fluids.

Carter [54] and Carter and Goddard [55] measured a non-zero first normal stress difference for suspensions of E-glass fibres (r = 57, 114, and 228; ϕ = 0.005–0.02) in a Newtonian polybutene oil (η_s = 18.6 Pa s). It was found that the results fitted well to Eq. (64), as seen in Fig. 1 which shows that the results reduce to a close group of parallel lines of slope unity on the log–log plot. Experimentally, the magnitude of normal stresses was of the order of a quarter of the shear stress. However, in the frequency range, ω = 0.24–2400 rad s^{-1}, no phase lag between the stress and strain

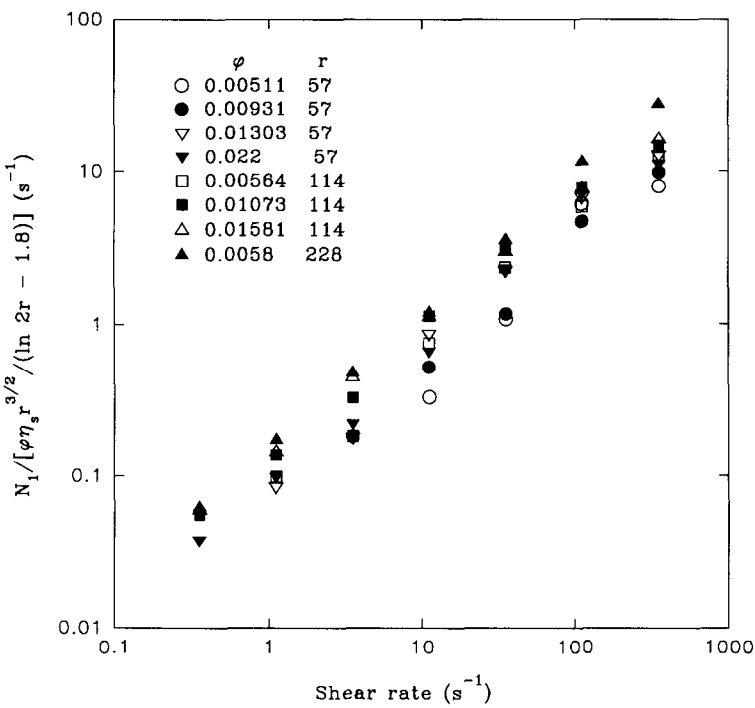

Fig. 1. $N_1/[\phi\eta_s r^{3/2}/(\ln 2r - 1.8)]$ versus shear rate for all first normal stress difference measurements of Carter [54]. In all cases the fibres were glass and η_s = 18.6 Pa s.

rate was detected for dynamic shear. Thus, the observed normal stresses at steady shear were considered not to be elastic properties of the suspension, but non-linear phenomena caused by the fibre interactions during flow, due to anisotropy in particle orientation and particle shape. It was believed that some, but not all, of the observed normal stress was due to wall effects. By use of unsteady shear tests and steady-plus-oscillatory shear tests it was also concluded that the suspensions studied were not elastic in their behaviour.

Christensen [56] observed first normal stress differences for suspensions of glass fibres with an aspect ratio of six suspended in wheat syrup ($\eta_s = 9.0$ Pa s). Below a fibre concentration of 0.29 v/v% no measurable first normal stress difference was observed. However, for fibre suspensions with fibre volume fractions between 0.29 and 1.035%, it was found that log–log plots of N_1 versus $\dot{\gamma}$ had a slope of unity and that the magnitude of N_1 increased with increasing fibre concentration. Christensen's results have been plotted in Fig. 2 as a log–log plot of $N_1/[\eta_s \phi r^{3/2}/(\ln 2r - 1.8)]$ versus shear rate to test the applicability of Carter's equation (64). It is found that the four sets of data reduce to two parallel lines of slope unity.

Kitano and Kataoka [61] observed that the first normal stress difference of suspensions of vinylon fibres ($r = 45.3$, 112.5 and 120.1) in silicone oil ($\eta_s = 100$ Pa s)

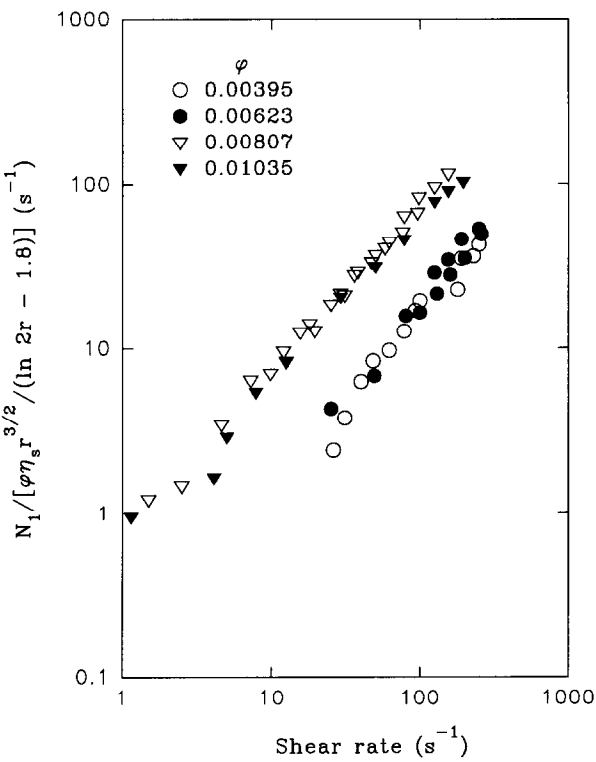

Fig. 2. $N_1/[\phi\eta_s r^{3/2}/(\ln 2r - 1.8)]$ versus shear rate for all first normal stress difference measurements of Christensen [56]. The fibres are glass, $r = 6$, and $\eta_s = 9.0$ Pa s in all cases.

increased with fibre concentration and aspect ratio. The slopes of the N_1 versus $\dot{\gamma}$ curves on log–log plots varied between 0.6 and 1.8, increasing with decreasing fibre concentration. A plot of characteristic time τ versus shear rate was presented, where τ is defined as

$$\tau = N_1/2\tau_{12}\dot{\gamma} \tag{65}$$

and where τ_{12} is the shear stress, and showed that τ decreased rapidly with the increase of shear rate for the suspensions. However, it should be noted that the solvent possessed a measurable N_1. Fig. 3 shows a log–log plot of $N_1/[\eta_s\phi r^{3/2}/(\ln 2r - 1.8)]$ versus shear rate for the results of Kitano and Kataoka [61] that were semi-dilute or close to semi-dilute (see Table 2). The N_1 used in the plot was taken as the difference between the suspension N_1 and the solvent N_1. The four data sets plotted fall into two groups, with the two data sets for fibres with $r = 45.3$ lying together with a slope of about unity, and those for $r = 112.5$ lying together with a slope of about 0.7.

Goto et al. [59] observed non-zero first normal stress differences for fibre suspensions where the aspect ratio of the fibres was greater than 100. Log–log plots of N_1 versus $\dot{\gamma}$ were straight lines with slopes that varied between 0.5 and 1.2. It was found for nylon fibres, at the same concentration, that an increase in aspect ratio increased the observed values of N_1, but decreased the value of the slope observed on the log–log plot. It was also found that increasing the concentration of fibres at a given aspect ratio had exactly the same effect. As fibre flexibility increased so did the observed values of N_1. An empirical equation of the form

$$N_1 = K_{11}\dot{\gamma}^s \tag{66}$$

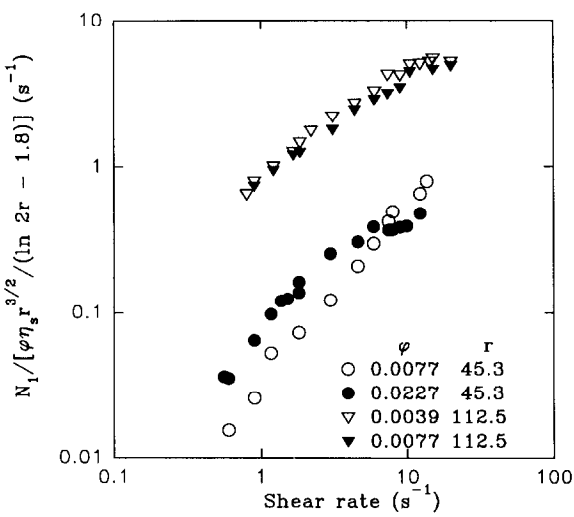

Fig. 3. $N_1/[\phi\eta_s r^{3/2}/(\ln 2r - 1.8)]$ versus shear rate for all N_1 measurements of Kitano and Kataoka [61]. The value of N_1 used here is the difference between the suspension N_1 and the solvent N_1. In all cases the fibres were vinylon and $\eta_s = 100$ Pa s.

Table 2
Concentration classification of the fibre suspensions used by Carter [54], Christensen [56], Kitano and Kataoka [61], and Goto et al. [59]

Reference	Fibre material	ϕ	r	r^{-2}	r^{-1}	Concentration classification
Data that fitted Eq. (64)						
Carter [54]	Glass	0.0051	57	0.00031	0.0175	Semi-dilute
		0.0093	57	0.00031	0.0175	Semi-dilute
		0.0130	57	0.00031	0.0175	Semi-dilute
		0.0220	57	0.00031	0.0175	Concentrated
		0.0056	114	0.00008	0.0087	Semi-dilute
		0.0107	114	0.00008	0.0087	Concentrated
		0.0158	114	0.00008	0.0087	Concentrated
		0.0058	228	0.00002	0.0044	Concentrated
Kitano and Kataoka [61]	Vinylon	0.0077	45	0.00049	0.0221	Semi-dilute
		0.0227	45	0.00049	0.0221	Concentrated
Goto et al. [59]	Carbon	0.0025	429	0.000005	0.0023	Concentrated
		0.0050	429	0.000005	0.0023	Concentrated
	Nylon	0.0100	100	0.0001	0.01	Semi-dilute
	Glass	0.0050	300	0.000011	0.0033	Concentrated
Data that did not fit Eq. (64)						
Christensen [56]	Glass	0.00395	6	0.02778	0.1667	Dilute
		0.00623	6	0.02778	0.1667	Dilute
		0.00807	6	0.02778	0.1667	Dilute
		0.01035	6	0.02778	0.1667	Dilute
Kitano and Kataoka [61]	Vinylon	0.0039	113	0.00008	0.0089	Semi-dilute
		0.0077	113	0.00008	0.0089	Semi-dilute
Goto et al. [59]	Nylon	0.0100	200	0.000025	0.0050	Concentrated
		0.0100	300	0.000011	0.0033	Concentrated
		0.0050	300	0.000011	0.0033	Concentrated
	Vinylon	0.0050	286	0.000012	0.0035	Concentrated

was fitted to the data obtained, where K_{11} and s were functions of the aspect ratio and volume fraction. In Fig. 4 the results are plotted as log–log of $N_1/[\eta_s \phi r^{3/2}/(\ln 2r - 1.8)]$ versus shear rate. The results for the "stiff" fibres, i.e. carbon, glass, and the lower aspect ratio nylon fibres, are grouped together in the plot having a slope of about unity, while the data sets for the more flexible fibres, higher aspect ratio nylon and vinylon fibres, lie scattered above the "stiff" fibre grouping and have slopes of about 0.5–0.6.

The $N_1[\eta_s \phi r^{3/2}/(\ln 2r - 1.8)]$ data of Carter [54], Kitano and Kataoka [61], and Goto et al. [59] that all lay within a narrow band have been plotted against shear rate in Fig. 5. The slope of the band is around unity on the log–log plot, as expected from Eq. (64), the constant K_{10} from the equation varying between 0.035 and 0.16 over the width of the band. Fig. 6 shows the data from Christensen [56],

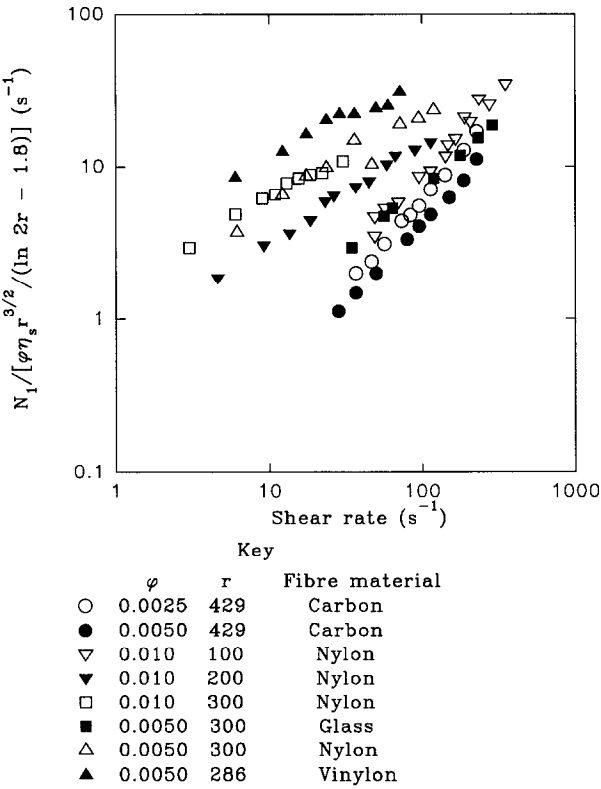

Fig. 4. $N_1/[\phi\eta_s r^{3/2}/(\ln 2r - 1.8)]$ versus shear rate for the first normal stress difference measurements of semi-dilute or close to semi-dilute suspensions of Goto et al. [59]. In all cases $\eta_s = 3.0$ Pa s.

Kitano and Kataoka [61] and Goto et al. [59] that did not lie within the band of Fig. 5. These data lie clumped together above the band.

Table 2 lists all the result sets plotted in Figs. 5 and 6 and classifies them, according to Eqs. (1)–(3), into dilute, semi-dilute and concentrated. Almost all the data classified as semi-dilute fall into the narrow band of Fig. 5. The fact that Christensen's results are for dilute suspensions and the fact the aspect ratio used was only six are probably the reasons why these data do not fit into the narrow band. It should be remembered that Eq. (64) was derived for large aspect ratios. The other data that do not lie in the band are all for fibres of very high aspect ratio (which are likely to be more flexible) and made from more flexible materials (nylon and vinylon). Hence it is probably the effect of flexibility that has caused the data to lie outside the band, and causes N_1 to vary with $\dot{\gamma}^n$ where n is less than unity and may vary with shear rate.

From a review of the available literature it is clear that the theories developed so far for dilute and semi-dilute fibre suspensions can adequately predict the experimentally observed suspension steady shear viscosity and elongational viscosity. The

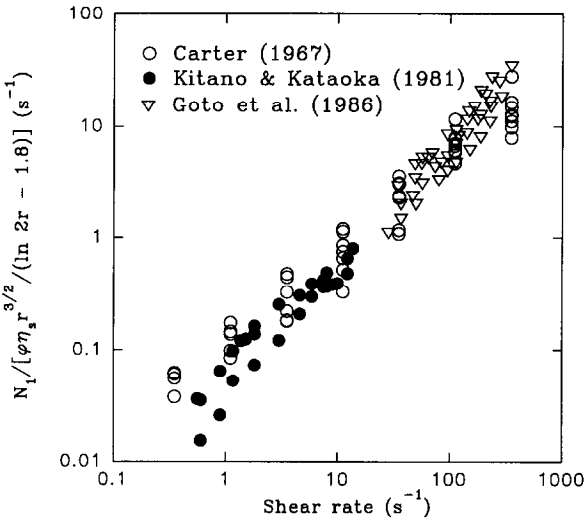

Fig. 5. Combined $N_1/[\phi\eta_s r^{3/2}/(\ln 2r - 1.8)]$ versus shear rate for the measurements of Carter [54], Kitano and Kataoka [61] and Goto et al. [59], showing only data that falls into a narrow band.

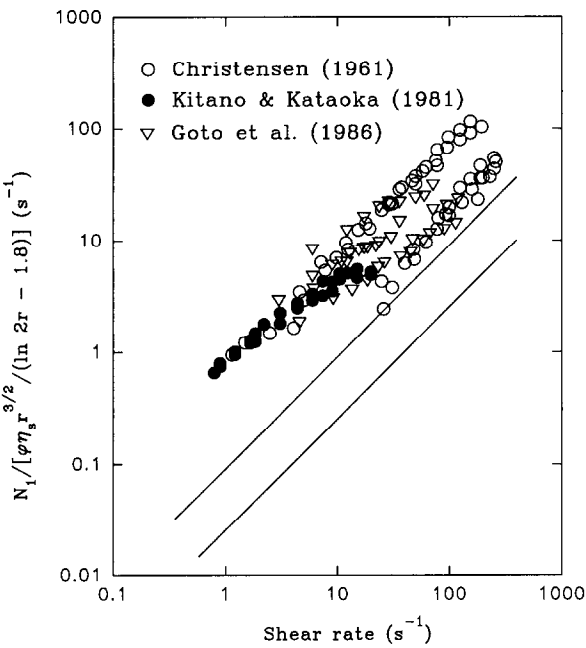

Fig. 6. Combined $N_1/[\phi\eta_s r^{3/2}/(\ln 2r - 1.8)]$ versus shear rate for the measurements of Christensen [56], Kitano and Kataoka [61] and Goto et al. [59], showing only data that does not fit Carter's theory [54]. The solid lines show the boundaries of the data from Fig. 5 which fitted the theory.

storage modulus of the dilute and semi-dilute fibre suspension is predicted and observed not to differ significantly from the storage modulus of the solvent, indicating that the fibres do not cause the suspension to become elastic. A number of experimental studies have observed first normal stress differences at steady state in non-dilute fibre suspensions, despite the fact that most theories predict negligible or zero first normal stress differences for such conditions. Much of the available experimental data fit the equation developed by Carter [54]. The experimental study which follows, the work having been carried out by Hur [87], aims to clearly define the relationship for first normal stress differences for constant viscosity semi-dilute fibre suspensions.

2. Experimental

The suspensions used were constructed from chopped glass fibres in Newtonian suspending fluids. The fluids were two grades of glucose wheat syrup, supplied by Fielder Gillespie Ltd., Melbourne, denoted MCY41N and MCY43N, with steady shear viscosities of 24.0 and 200.0 Pa s respectively at 20°C, and an epoxy resin, Epikote 828 from Shell Chemical, with a steady shear viscosity of 28.0 Pa s at 20°C. The fibres used were 3.2 mm (1/8″) and 6.4 mm (1/4″) chopped S-glass supplied by Owens-Corning-Fiberglas. The sizing on fibre bundles was removed by leaving the fibre bundles to soak overnight in an organic solvent (typically *n*-hexane), and then heating to 450°C for two hours in a muffle furnace. The aspect ratio of individual fibres after separation of the bundles was 276 for 3.2 mm fibres and 552 for 6.4 mm fibres. Suspensions were prepared by adding a weighted quantity of fibres to the suspending fluid and stirring gently with a helical-ribbon impeller until complete dispersion was achieved. The suspensions were kept overnight at 50°C to ensure removal of entrapped air bubbles. The initial state of complete dispersion could be maintained for several days by additional stirring without fibre breakage.

Viscosity and first normal stress difference measurements were carried out on a Weissenberg Rheogoniometer model R-19 in a cone-and-plate configuration, using a large (4.5°) cone angle. Parallel-plate geometry was also used. The viscosity data were confirmed by using a capillary rheometer and a Haake model RV-3 Couette viscometer [87,88].

During the shear stress measurement of wheat syrup based fluids using the cone-and-plate configuration of the Rheogoniometer, evaporation effects [89] were minimised by applying a thin film of inert silicone oil of comparable viscosity to the exposed surface of the test fluid.

3. Results

3.1. *Weissenberg effect*

For the fibre suspensions constructed, significant rod-climbing phenomena were observed around a rotating shaft during the mixing process. Fig. 7 shows a typical

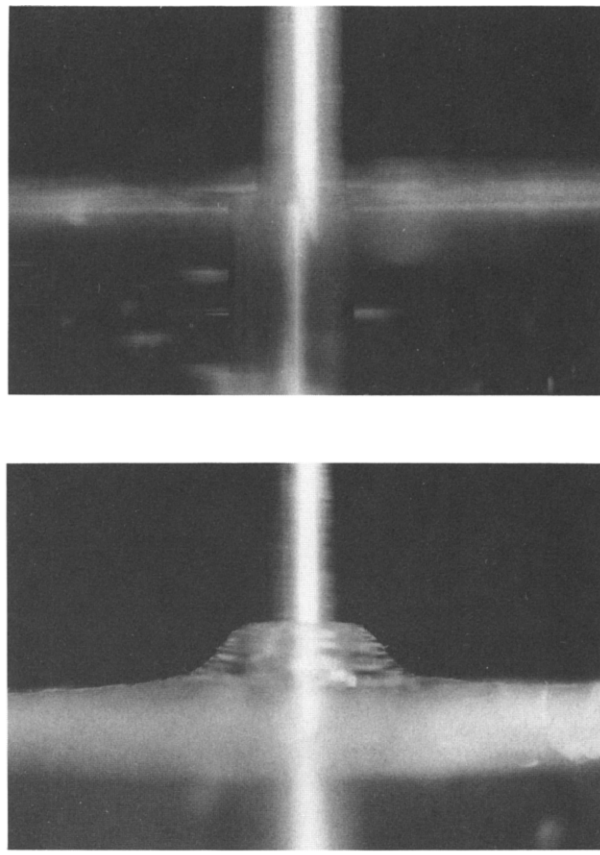

(a)

(b)

Fig. 7. The Weissenberg effect for a semi-dilute glass fibre suspension in a Newtonian wheat syrup, MCY41N. (a) Newtonian suspending fluid, MCY41N; (b) 0.045 v/v% 3 2 mm fibres in MCY41N.

Weissenberg effect for a semi-dilute fibre suspension in a Newtonian fluid: $\phi = 0.045$ v/v%, $r = 276$ and 540 r.p.m., in comparison with the Newtonian suspending fluid. The rise in height of the fibre suspension on the rod in steady rotation was oscillatory. At low rotational velocities, the shape of the free surface of the climbing suspension was axisymmetric, but became asymmetric with increasing rotational speed. However, the mean rise was strongly dependent on the fibre concentration, fibre aspect ratio, viscosity of suspending fluid, and the diameter of the shaft. The shape of the free surface was dependent on the shaft diameter, being more convex as the ratio of shaft diameter to fibre length increased and vice versa. When the viscosity of the suspending fluid was lowered, the rod-climbing effect was decreased. The Weissenberg effect observed for the semi-dilute fibre suspensions illustrates the presence of normal stresses due to the particle anisotropy and interaction-dependent orientations, rather than the more conventional elastic effect observed with flexible polymer solutions.

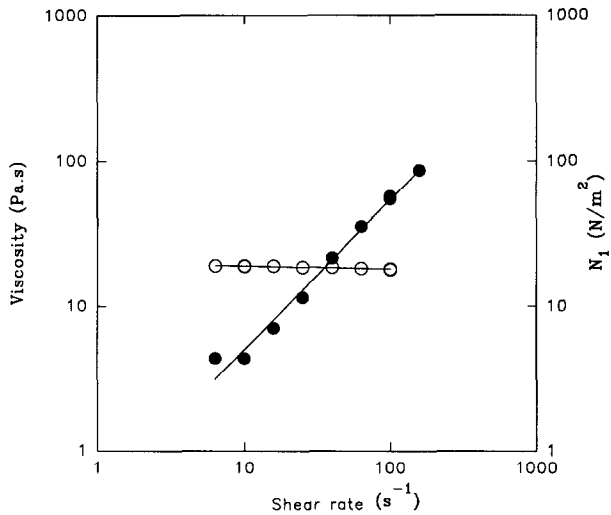

Fig. 8. Steady shear properties of 0.0299 v/v% 3.2 mm fibres ($r = 276$) in MCY41N at 22.5°C.

3.2. *Rheological properties of semi-dilute fibre suspensions*

Fig. 8 shows a typical result of suspension viscosity and first normal stress difference, N_1, as a function of shear rate, $\dot{\gamma}$, for a suspension of 0.0299 v/v% 3.2 mm fibres in MCY41N at 22.5°C. The N_1 versus $\dot{\gamma}$ line has a slope of unity. The suspension viscosity is only slightly increased above that of the suspending medium and shows a very small amount of shear thinning.

In Fig. 9 the effect of fibre concentration upon the observed first normal stress difference is shown. Increasing the fibre concentration increased the magnitude of N_1 while the slope of the line remained approximately unity. Deviations from the slope of unity are believed to be due to experimental uncertainties. All the suspensions in Fig. 9 were in the semi-dilute region, as defined by Eq. (2). In the semi-dilute region the shear viscosity is essentially unaffected by the presence of fibres as predicted by the continuum theory [27,81,82], whereas the first normal stress difference increases rapidly with fibre volume concentration. The minimum fibre concentration at which measurable N_1 was obtained in a cone-and-plate apparatus was 0.02 v/v% or $\phi r^2 = 15$. This concentration is an order higher than the critical value, $\phi r^2 = O(1)$, where fibre interactions (i.e. collision-dependent fibre orientations) become significant enough to give rise to normal stresses. Therefore, it is clear that the measured N_1 of the semi-dilute fibre suspensions might be caused by the flow-induced anisotropy in fibre orientation distributions due to the particle interactions, or the wall effect, or both.

Fig. 10 shows the dimensionless first normal stress difference, N_1/τ_{12}, as a function of volumetric fibre concentration for a fixed fibre aspect ratio of 276 and at constant shear stress, $\tau_{12} = 1000$ N m^{-2}. There is a linear relationship between

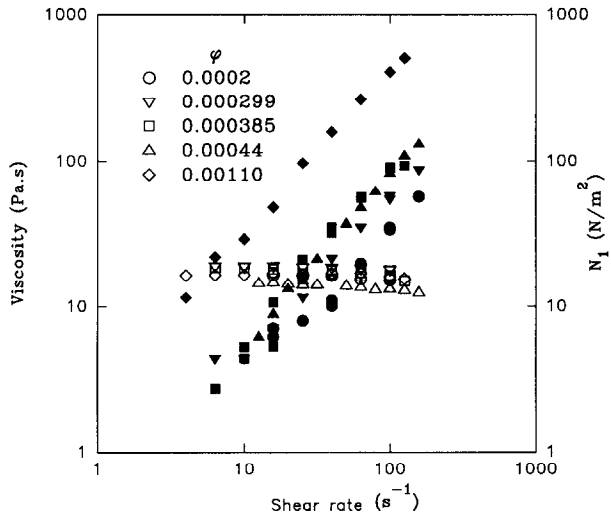

Fig. 9. Steady shear viscosity and first normal stress difference as a function of shear rate for suspensions of 3.2 mm glass fibres ($r = 276$) at different concentrations in MCY41N at 22.5°C.

N_1/τ_{12} and ϕ. It will be noted that the line does not extend through the origin as might be expected. However, it should also be noted that significant fibre–fibre interactions are necessary for normal stresses to arise and thus the first normal stress difference will be effectively zero at some non-zero fibre concentration. The linear relationship between N_1 and ϕ is predicted by Carter [54], Brenner [3], and Doi and Edwards [47].

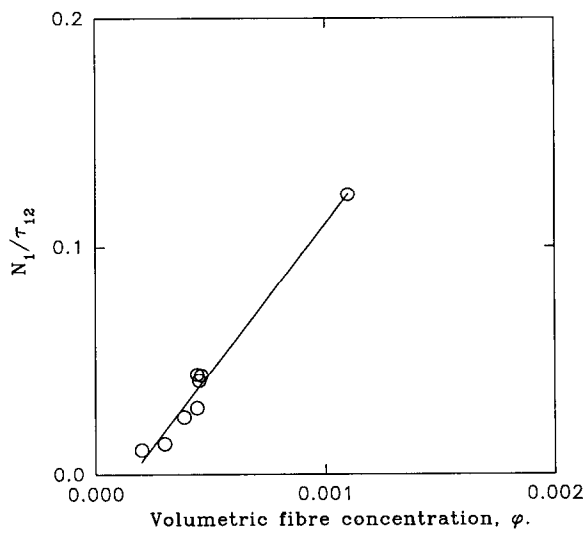

Fig. 10. Linear dependence of dimensionless first normal stress difference upon volumetric fibre concentration for constant fibre aspect ratio, $r = 276$, and shear stress $\tau_{12} = 1000$ N m^{-2}.

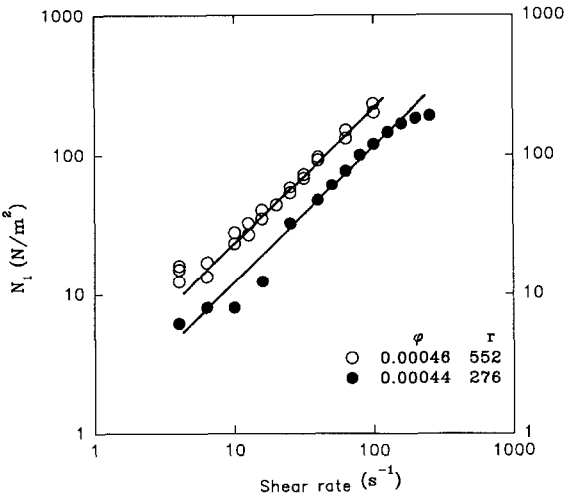

Fig. 11. Effect of fibre aspect ratio on first normal stress difference for two fibre suspensions with the same fibre volumetric concentration.

The effect of fibre aspect ratio, r, on the first normal stress difference is shown in Fig. 11. An increase in the fibre aspect ratio caused the magnitude of N_1 to increase, but once again the slope on the log–log plot remained around unity.

Fig. 12 shows twice the storage modulus, $2G'$, of 0.04 v/v%, 3.2 mm glass fibres in the Epikote 828 resin in comparison with that of the Newtonian suspending fluid and the N_1 of the same fibre suspension. There was no significant difference in the

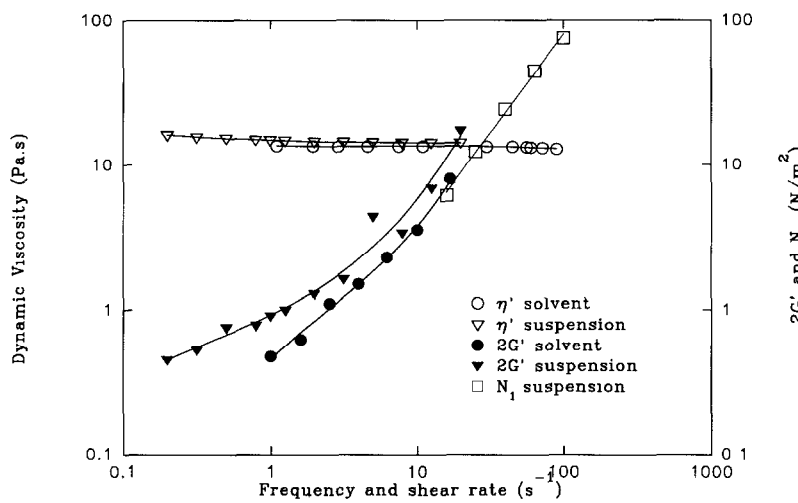

Fig. 12. Dynamic viscosity and $2G'$ of 0.04 v/v% 3.2 mm fibres ($r = 276$) in Epikote 828 resin at 22.5°C in comparison with those of the Newtonian epoxy resin solvent and the N_1 of the suspension.

storage modulus and the viscosity between the fibre suspension and Newtonian suspending fluid, whereas finite normal stress difference was observed for the suspension, which is approximately linear with shear rate. This observation implies that the first normal stress difference measured for the fibre suspension is simply a manifestation of the non-linear effects due to fibres rather than fluid elasticity as in dilute solutions of flexible polymer molecules.

It was found that the measured N_1 for the suspensions is not dependent upon the direction of shear (i.e. forward or backward).

The first normal stress difference significantly decreased with increase of total strain, $\dot{\gamma}t$, which is an indirect measure of fibre breakage during the shearing in 4.5° cone-and-plate geometry. Fig. 13 illustrates a decrease in N_1 due to the effects of shear strain on fibre breakage for 6.4 mm glass fibres at $\phi = 0.044$ v/v% during the shearing in the cone-and-plate at $\dot{\gamma} = 10\ s^{-1}$ for one hour ($\dot{\gamma}t = 3.6 \times 10^4$). For other fibre suspensions used in this work the fibre breakage is not considered to be significant enough to affect N_1 measurements, since the applied total strain was usually much less than the above value and most suspensions were of the shorter fibres where breakage is less.

In Fig. 14 the first normal stress difference is shown as a function of shear stress and temperature for 0.110 v/v% 3.2 mm glass fibres in MCY41N. The slope of the experimental data on the logarithmic coordinates has a value of about unity. Thus, the stress ratio, N_1/τ_{12}, of the semi-dilute fibre suspension is essentially independent of the temperature within the range studied, i.e. 20–25°C. In contrast, the viscosity of the Newtonian suspending fluid is very temperature dependent, varying from 24 Pa s at 22°C to 12 Pa s at 26°C.

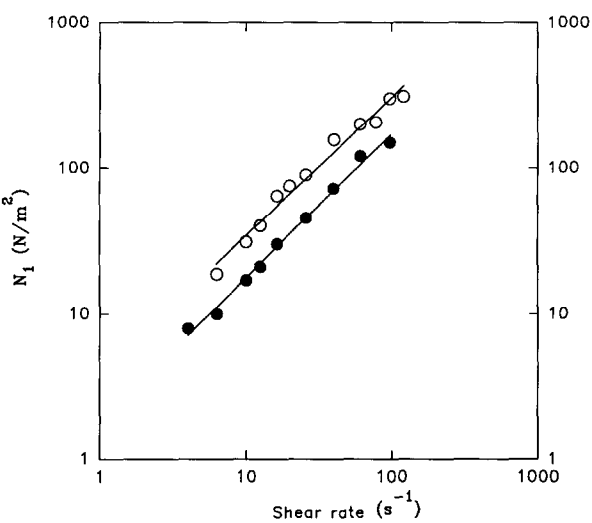

Fig. 13. Illustration of decrease in N_1 in a fibre suspension due to fibre breakage as a result of large total strain. (○) N_1 initially for 0.044 v/v% 6.4 mm glass fibres ($r = 552$) in MCY41N at 19.5°C; (●) N_1 after additional shear at a shear rate of 10 s^{-1} for one hour.

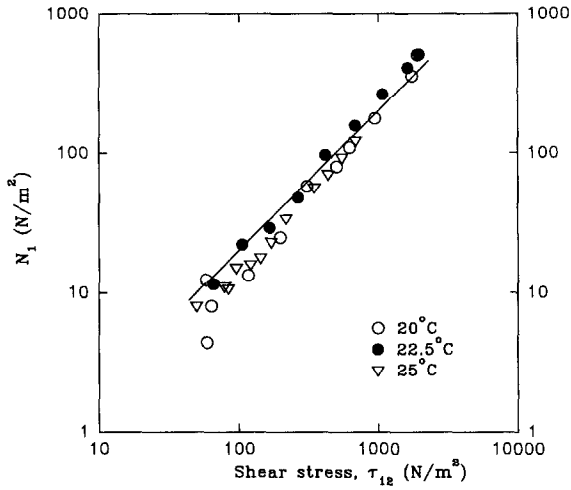

Fig. 14. First normal stress difference as a function of shear stress and temperature for 0.110 v/v% 3.2 mm glass fibres in MCY41N, showing the temperature independent stress ratio, N_1/τ_{12}.

The influence of Newtonian solvent viscosity on N_1 was also investigated. As shown in Fig. 15, when the solvent viscosity was increased about eight-fold, N_1 increased by a factor of two at most, in the shear rate range from 10 to 50 s^{-1}. The results conflict with theory, as Carter [54] predicts a linear dependence of N_1 on η_s, and Hinch and Leal [13], Brenner [3], and Mackay [84] predict that N_1 is independent of η_s. For Hinch and Leal's equation (55), it should be noted that the η_s shown in the equation will cancel the η_s in D_r.

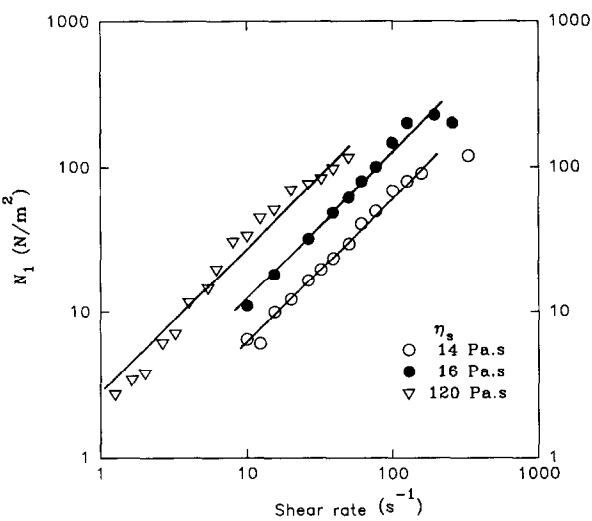

Fig. 15. First normal stress difference as a function of shear rate for 0.044 v/v% 3.2 mm glass fibres ($r = 276$) in Newtonian fluids at 22.5°C, illustrating the dependence of N_1 on solvent viscosity.

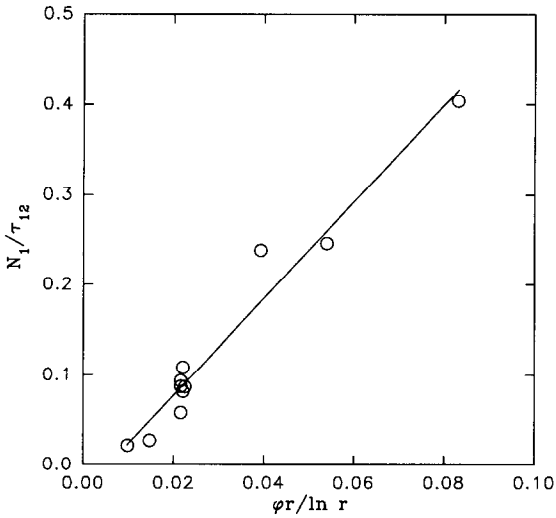

Fig. 16. Linear dependence of the dimensionless first normal stress difference on $\phi r/\ln r$ at a constant shear stress, $\tau_{12} = 1000$ N m^{-2}.

In Fig. 16 the dimensionless first normal stress difference, N_1/τ_{12}, at constant shear stress, $\tau_{12} = 1000$ N m^{-2}, is plotted as a function of fibre volume fraction, ϕ, multiplied by a dimensionless parameter depending on the fibre aspect ratio, r, given as $\phi r/\ln r$, for all the 3.2 and 6.4 mm glass fibre suspensions at volume fractions of 0.110 v/v% or less. The parameter $\phi r/\ln r$ was selected as it comes out of Lipscomb's [81,82] continuum theory for fibre suspensions. Correlation between N_1/τ_{12} and $\phi r/\ln r$ is good with some deviation from linearity at low volume fractions. However, it should be remembered that only two aspect ratios of fibres were used in this work. Theoretical predictions [14,27,81,82,90] and the experimental results of this work show that the increase in the bulk shear stress is almost negligible for dilute and semi-dilute fibre suspensions in a Newtonian fluid so that $\tau_{12} \approx \eta_s \dot{\gamma}$ (or $\eta \approx \eta_s$). Thus N_1/τ_{12} is relatively constant regardless of the shear rate as both the shear stress and the first normal stress difference are linearly dependent on the shear rate. As with Fig. 10 it should not be expected that the line will pass through the origin. According to Lipscomb et al. [81] and Lipscomb [82] the linear dependence of N_1/τ_{12} on the parameter $\phi r/\ln r$ is only valid when $t^*(=\dot{\gamma}t/r) = O(1)$, but at steady state ($t^* \to \infty$) N_1 is predicted to be zero.

In Fig. 17 N_1/τ_{12} is plotted versus Carter's [54,55] parameter, $\phi r^{3/2}/(\ln 2r - 1.8)$, that appears in Eq. (64), at constant shear stress, $\tau_{12} = 1000$ N m^{-2}. The correlation between N_1/τ_{12} and $\phi r^{3/2}/(\ln 2r - 1.8)$ is excellent. In this case the solvent viscosity as a variable has been ignored, as Fig. 15 indicated that Carter's prediction that N_1 varies linearly with η_s does not hold for the suspensions used, for which the solvent viscosity varied.

In Fig. 18 $N_1/[\eta_s \phi r^{3/2}/(\ln 2r - 1.8)]$ is plotted versus the shear rate for all the fibre suspensions used in this study. These results are compared with the band of

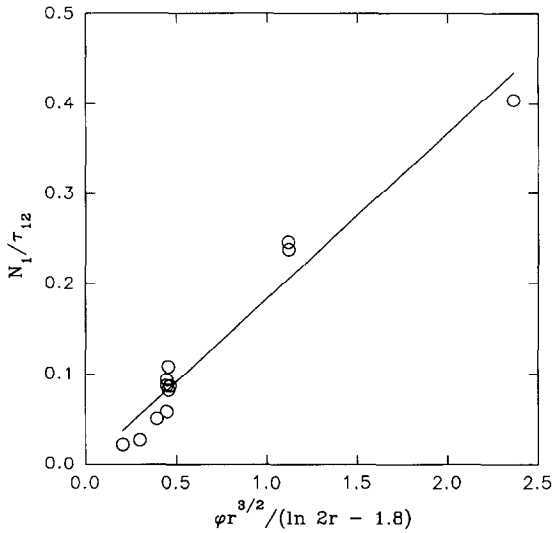

Fig. 17. Linear dependence of the dimensionless first normal stress difference on $\phi r^{3/2}/(\ln 2r - 1.8)$ at a constant shear stress, $\tau_{12} = 1000$ N m^{-2}.

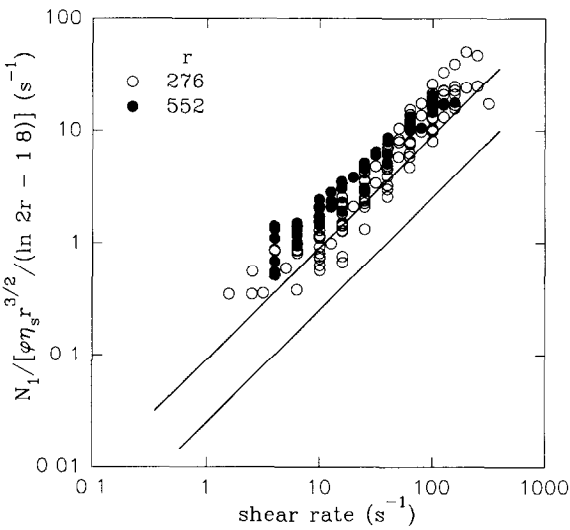

Fig 18. $N_1/[\phi\eta_s r^{3/2}/(\ln 2r - 1.8)]$ versus shear rate for all the glass fibre suspensions used in this work. The suspensions of fibres with $r = 276$ had volume fractions between 0.020 and 0.110 vv%, while those with $r = 552$ had volume fractions between 0.045 and 0.095 v/v%. The solid lines show the upper and lower boundaries of the data of Carter [54], Kitano and Kataoka [61] and Goto et al. [59] that were taken to fit Carter's theory [54] (see Fig. 5).

results that were taken to fit Carter's theory [54] in Fig. 5. The results fall within a band, with some results lying within the band from Fig. 5, but with most results falling just outside the band on the high side. Using Carter's equation (64), the value of the constant K_{10} varies between 0.082 and 0.27 for the results in Fig. 18, which is a slightly wider variation than the results for Fig. 5. The fact that many results lie outside the band of results in Fig. 5 and that there is a wider variation in the results, is believed to be due to the effect of the differences in solvent viscosity of the suspensions and the effect the solvent viscosity may have on the flexibility of the fibres.

3.3. First normal stress difference measurements using parallel-plate geometry

The major advantage of the cone-and-plate apparatus for rheological measurements on unfilled non-Newtonian fluids is that it provides an essentially uniform shear rate throughout the sheared sample. To achieve the condition of uniform shear rate with minimal effects, i.e. secondary flows, the cone angle is kept small ($\alpha < 2-5°$) and the gap setting (Δ) between the cone and plate is correspondingly very narrow. For one of the cones used in this work, with a cone angle of 4.5°, the gap distance varies from 0.19 mm at the centre to 2.95 mm at the rim. However, for suspensions of glass fibres of large aspect ratio ($r > 10$, or $L > 0.1$ mm), the gap distance must be large in comparison to the fibre length to minimise the possibilities of wall effects [23,91], the instability of the suspension when under shear (where the suspension becomes separated from the upper plate at the plate edges [54,55]), and other experimental difficulties associated with fibre breakage and fibre interlocking. Thus in this work, the parallel-plate geometry was used in addition to the cone-and-plate geometry to evaluate wall effects. The parallel-plate geometry has the disadvantage that the shear rate between the two parallel plates is no longer uniform, but is strongly dependent upon the radial position. The use of parallel-plate geometry gives a normal stress that is the difference between the first normal stress difference and the second normal stress difference [92].

To examine the validity and accuracy of the parallel-plate method, in the measurement of normal stresses, two polydimethyl siloxanes, disignated as a 12 500 cSt fluid and a 30 000 cSt fluid, respectively, were used as weakly elastic non-Newtonian test fluids. It was found that there was excellent agreement between the observed normal stress difference from parallel-plate geometry, at a radius of 3.75 cm and gap settings of 0.5, 1.0, and 1.5 mm, and the first normal stress difference measured by the cone-and-plate geometry, with a cone angle of 2.47° [87]. This suggests that the second normal stress difference for the fluids was small, and thus it will be assumed that $N_1 \gg N_2$, where N_2 is the second normal stress difference. Thus the normal stress difference measured by parallel-plate geometry will be taken to be the first normal stress difference.

Fig. 19 shows the data obtained with the parallel-plate apparatus for a semi-dilute fibre suspension in a polybutene oil (Hyvis 03); $\phi = 0.10$ v/v%, $r = 276$, and $\eta_0 = 6.9$ Pa s at 20°C. For gap settings up to 2.5 mm no significant deviation from linearity was found when the data were plotted on the logarithmic coordinates.

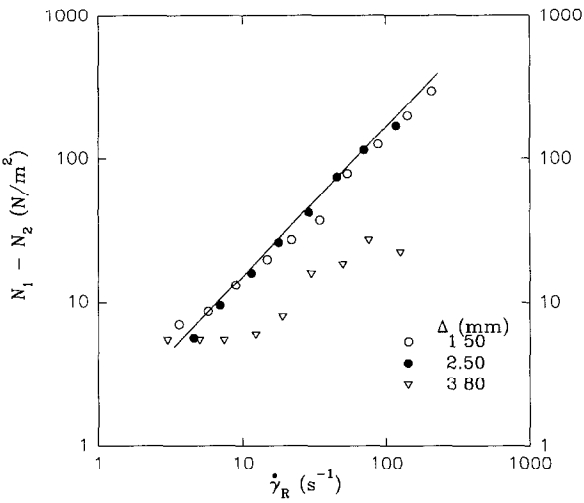

Fig. 19. Dependence of $(N_1 - N_2)$ on gap distance (Δ) of the parallel plates for a 0.10 v/v% 3.2 mm glass fibre ($r = 276$) in polybutene oil suspension at 20.0°C. The solid line represents the cone-and-plate data.

However, at the gap setting $\Delta = 3.8$ mm, which is larger than the fibre length, $L = 3.2$ mm, the fibre suspension showed a non-linearity that was pronounced even at the lowest shear rates used, $\dot{\gamma}_R \geqslant 5.0$ s^{-1}, where $\dot{\gamma}_R$ is the shear rate at a radius of 3.75 cm. As the shear rate increased further, $\dot{\gamma}_R > 10$ s^{-1}, the sample expanded significantly so as to show irregular free surface around the gap, and eventually separated from the gap. This separation effect was dependent upon both the gap spacing and the viscosity of the suspending fluid.

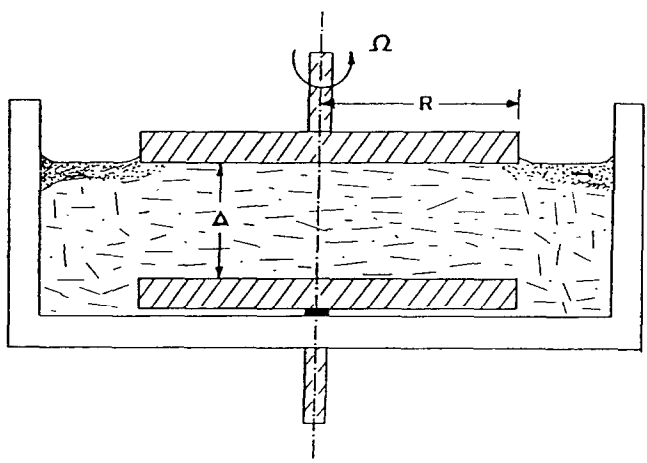

Fig. 20. Parallel-plate geometry with a sample bath for measurement of the rheological properties of fibre suspensions.

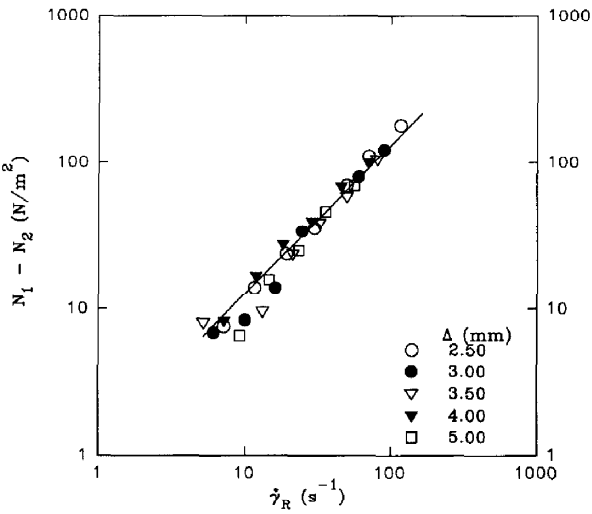

Fig. 21. Independence of $(N_1 - N_2)$ on the gap distance (Δ) of the parallel plates with a sample bath for a 0.10 v/v% 3.2 mm glass fibre ($r = 276$) in polybutene oil suspension at 20.0°C. The solid line represents data obtained using cone-and-plate geometry.

In order to minimise the flow instability and the separation effect, the parallel-plate apparatus was modified by immersing the parallel plates in a sample bath as depicted in Fig. 20. As a result, the shear rate was successfully extended up to 100 s^{-1} without serious difficulties such as flow instability, sample separation, or fibre breakage.

Fig. 21 illustrates the rheological measurements with parallel-plate apparatus immersed in the sample bath at 20°C for the same fibre suspension used in Fig. 19 without the bath device. There was no indication of sample separation nor flow instability at higher shear rates ($5\ s^{-1} < \dot{\gamma}_R < 100\ s^{-1}$), although the gap settings were doubled ($2.5\ mm \leqslant \Delta \leqslant 5.0\ mm$), ranging from 0.8 times to 1.6 times the fibre length. The shear stress and normal stress difference data for 2.5, 3.0, 3.5, 4.0 and 5.0 mm gap settings were approximately coincident lying on a straight line of slope 1.0. However, there was a tendency for the shear stress to increase slightly with increasing gap setting, while the normal stress was rather scattered, particularly at low shear rates. The gap setting was not increased beyond 5.0 mm, in order to minimise the possibilities of slip effects between the upper plate and the suspension sample, and of secondary flow around the rim. These results are consistent with the prediction that N_1 varies linearly with $\dot{\gamma}$ for flow between two parallel plates as given in Mackay's [84] equation (63); however, the predicted dependence of N_1 on Δ^2 is not observed.

To confirm these findings the rheological properties of a semi-dilute fibre suspension, $\phi = 0.046$ v/v% and $r = 276$, in a wheat syrup ($\eta_0 = 24$ Pa s at 20°C) were measured using the same procedure. In order to reduce the evaporation effect [89], a thin-film of silicone oil of comparable viscosity was applied to the free

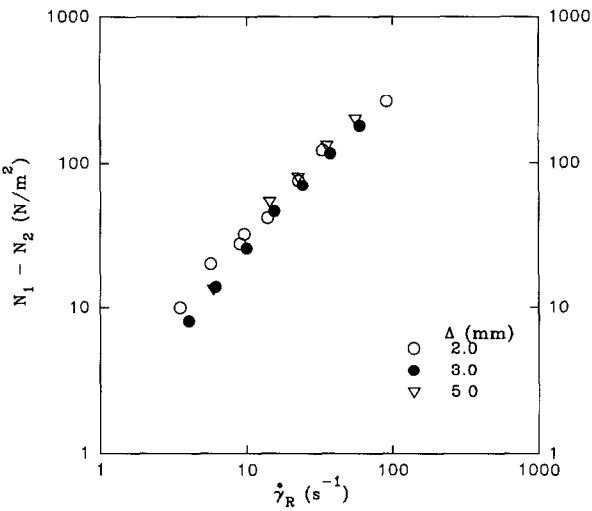

Fig. 22. Independence of $(N_1 - N_2)$ on gap distance (Δ) of the parallel plates with a sample bath for a 0.046 v/v% 3.2 mm glass fibre ($r = 276$) in MCY41N suspension at 20.0°C.

surface of the fibre suspension sample. The normal stress difference, $(N_1 - N_2)$, is presented as a function of the gap setting and shear rate in Fig. 22. The results show, as before, that the normal stress difference data are independent of the gap setting within the range examined, and also vary linearly with $\dot{\gamma}_R$.

The fact that no wall effects were observed using either the cone-and-plate geometry or parallel-plate geometry confirms the earlier statement that during the measurement of the rheological properties the fibres become aligned, and hence the diameter is the most important fibre dimension, which is much smaller than the characteristic dimension of the measuring apparatus [28].

4. Conclusions

A review of the theories relating to fibres suspended in Newtonian fluids showed that continuum theory is able to account for the increase in viscosity for dilute and semi-dilute fibre suspensions over that of the suspending fluid. Theory also correctly predicts that this viscosity increases with increasing fibre concentration. The shear thinning shown by more concentrated fibre suspensions, or those in which the fibre aspect ratio is large, has also been predicted by some theories. However, as of yet there does not appear to be one single definitive equation for the relative viscosity of dilute and semi-dilute fibre suspensions in Newtonian flows that will predict all the available experimental data.

Theory has correctly predicted a constant extensional viscosity with elongational strain for non-dilute fibre suspensions which is large compared to the extensional viscosity of the Newtonian suspending fluid [26,71,72].

Experimentally it has been found that the normal stresses are approximately linear with shear rate and fibre concentration and increase in magnitude with fibre flexibility. As there was no observed phase lag between the stress and strain rate in dynamic shear for such suspensions, the normal stresses are not elastic properties of the suspension. Thus the normal stresses arise from fibre–fibre interactions and wall effects, causing anisotropy in particle orientation.

Continuum theories do not agree upon the prediction of normal forces in non-dilute fibre suspensions. In fact, many continuum theories predict that the normal stress is zero at steady state. However, as confirmed by the work done in this paper, the theory developed by Carter [54] adequately predicts the dependence of the first normal stress difference upon the parameter $\phi r^{3/2}/(\ln 2r - 1.8)$ and that the first normal stress difference increases linearly with shear rate. However, the experimental results of Hur [87] do not agree with Carter's prediction that first normal stress difference depends linearly upon solvent viscosity, and hence further work needs to be done to investigate the relationship between the two.

Small changes in temperature do not greatly affect the observed normal stress.

A system of parallel-plate geometry immersed in a sample bath offers a useful method of measuring the rheological properties of fibre suspensions while minimising wall effects.

Acknowledgement

Fundamental research in non-Newtonian fluid mechanics at the University of Melbourne is supported by the Australian Research Council. The authors are grateful for their continuing support.

References

[1] L. Ganani and R.L. Powell, Suspensions of rodlike particles: literature review and data correlations, J. Compos. Mater., 19 (1985) 194–215.

[2] G.B. Jeffery, The motion of ellipsoidal particles immersed in a viscous fluid, Proc. R. Soc. London, Ser. A, 102 (1922) 161–179.

[3] H. Brenner, Rheology of a dilute suspension of axisymmetric Brownian particles, Int. J. Multiphase Flow, 1 (1974) 195–341.

[4] M. Doi and S.F. Edwards, Dynamics of rod-like macromolecules in concentrated solution. Part 1, J. Chem. Soc., Faraday Trans. 2, 74 (1978) 560–570.

[5] J.M. Burgers, On the Motion of Small Particles of Elongated Form, Suspended in a Viscous Liquid, in Second Report on Viscosity and Plasticity, Chapter 3, North-Holland, Amsterdam, 1938; Kon. Ned. Akad. Wet., Verhand, (Erste Sectie), 16(4) 113–184.

[6] A. Okagawa, R.G. Cox and S.G. Mason, The kinetics of flowing dispersions. VI: Transient orientation and rheological phenomena of rods and discs in shear flow, J. Colloid Interface Sci., 45 (1973) 303–329.

[7] E. Anczurowski and S.G. Mason, The kinetics of flowing dispersions, III: Equilibrium orientations of rods and discs (experimental), J. Colloid Interface Sci., 23 (1967) 533–546.

[8] E. Anczurowski and R.G. Cox, The kinetics of flowing dispersions. IV: Transient orientations of cylinders, J. Colloid Interface Sci., 23 (1967) 547–562.

[9] P.A. Arp and S.G. Mason, Interactions between two rods in shear flow, J. Colloid Interface Sci., 59 (1977) 378–380.
[10] P. Brunn, The motion of rigid particles in viscoelastic fluids, J. Non-Newtonian Fluid Mech., 7 (1980) 271–288.
[11] F. Folgar, Fibre Orientation Distribution in Concentrated Suspensions: A Predictive Model, Ph.D. Thesis, University of Illinois at Urbana-Champaign, USA, 1983.
[12] H. Giesekus, Die simultane Translations- und Rotationsbewegung einer Kugel in einer elastoviskosen Flüssigkeit, Rheol. Acta, 3 (1963) 59–71.
[13] E.J. Hinch and L.G. Leal, The effect of Brownian motion on the rheological properties of a suspension of non-spherical particles, J. Fluid Mech., 52 (1972) 683–712.
[14] E.J. Hinch and L.G Leal, Time-dependent shear flows of a suspension of particles with weak Brownian rotations, J. Fluid Mech., 57 (1973) 753–767.
[15] E.J. Hinch and L.G. Leal, Constitutive equations in suspension mechanics, Part 2. Approximate forms for a suspension of rigid particles affected by Brownian rotations, J. Fluid Mech., 76 (1976) 187–208.
[16] Y. Ivanov, T.G.M. van de Ven and S.G. Mason, Damped oscillations in the viscosity of suspensions of rigid rods. I: Monomodal suspensions, J. Rheol., 26 (1982) 213–230.
[17] Y. Ivanov, T.G.M. van de Ven and S.G. Mason, Damped oscillations in the viscosity of suspensions of rigid rods. II: Bimodal and polydisperse suspensions, J. Rheol., 26 (1982) 231–244.
[18] A. Karnis, H.L. Goldsmith and S.G. Mason, The kinetics of flowing dispersions. I. Concentrated suspensions of rigid particles, J. Colloid Interface Sci., 22 (1966) 531–553.
[19] S.G. Mason and R.St.J. Manley, Particle motions in sheared suspensions: orientations and interactions of rigid rods, Proc. R. Soc. London, Ser. A, 238 (1957) 117–131.
[20] A. Okagawa, R.G. Cox and S.G. Mason, The kinetics of flowing dispersions. XII: Some effects of nonuniform shear, J. Colloid Interface Sci., 71 (1979) 11–17.
[21] N. Phan-Thien, The effects of Random Initial Orientation and Random Aspect Ratio on the Stress Induced by Rotating Spheroidal Particles in a Shear Flow, private communication, 1986.
[22] C.A. Stover, D.L. Koch and C. Cohen, Observations of fibre orientation in simple shear flow of semi-dilute suspensions, J. Fluid Mech., 238 (1992) 277–296.
[23] M.A. Bibbo, S.M. Dinh and R.C. Armstrong, Shear flow properties of semi-concentrated fibre suspensions, J. Rheol., 29 (1985) 905–929.
[24] A. Okagawa and S.G. Mason, The kinetics of flowing dispersions. VII: Oscillatory behaviour of rods and discs in shear flow, J. Colloid Interface Sci., 45 (1973) 330–358.
[25] G.K. Batchelor, The stress system in a suspension of force-free particles, J. Fluid Mech., 41 (1970) 545–570.
[26] G.K. Batchelor, The stress generated in a non-dilute suspension of elongated particles by pure straining motion, J. Fluid Mech., 46 (1971) 813–829.
[27] S.M. Dinh and R.C. Armstrong, A rheological equation of state for semi-concentrated fibre suspensions, J. Rheol., 28 (1984) 207–227.
[28] R.L. Powell, Rheology of suspensions of rodlike particles, J. Stat. Phys., 62 (1991) 1073–1094.
[29] R.O. Maschmeyer, Rheology of Concentrated Suspensions of Fibres, Ph.D. Dissertation, Washington University, Seattle, WA, 1974.
[30] E. Guth, On the theory of the viscosity of suspensions of ellipsoidal particles, Phys. Rev., 53 (1938) 926.
[31] R. Eisenschitz, Die Viskosität von Suspensionen Laggestreckter Teilchen und ihre Interpretation durch Raumbeanspruchung, Z. Phys. Chem., Abt. A, 158 (1932) 78–90.
[32] R. Eisenschitz, Die Einfluss der Brownschen Bewegung auf die Viscosität von Suspension, Z. Phys. Chem., Abt. A, 163 (1933) 133–141.
[33] R. Simha, The influence of Brownian movement on the viscosity of solutions, J. Phys. Chem., 44 (1940) 25–34.
[34] W. Kuhn and H. Kuhn, Die Abhängigkeit der Viskosität vom Strömungsgefälle bei hochverdünnten Suspensionen and Losungen, Helv. Chim. Acta., 28 (1945) 97–127.

[35] H.A. Scheraga, Non-Newtonian viscosity of solutions of ellipsoidal particles, J. Chem. Phys., 23 (1955) 1526–1532.
[36] M.A. Nawab and S.G. Mason, The viscosity of dilute suspensions of thread-like particles, J. Phys. Chem., 62 (1958) 1248–1253.
[37] J.G. Brodnyan, The concentration dependence of the Newtonian viscosity of prolate ellipsoids, Trans. Soc. Rheol., 3 (1959) 61–68.
[38] W.R. Blakeney, The viscosity of suspensions of straight rigid rods, J. Colloid Interface Sci., 22 (1966) 324–330.
[39] K.D. Ziegel, The viscosity of suspensions of large nonspherical particles in polymer fluids, J. Colloid Interface Sci., 34 (1970) 185–196.
[40] L.G. Leal and E.J. Hinch, The effect of weak Brownian rotations on particles in shear flow, J. Fluid Mech., 46 (1971) 685–703.
[41] R.F. Fedors, Relationship between viscosity and concentration for Newtonian suspensions, J. Colloid Interface Sci., 46 (1974) 545–547.
[42] R.F. Fedors, Viscosity of Newtonian suspensions, Polymer, 16 (1975) 305–306.
[43] R.O. Maschmeyer and C.T. Hill, Rheology of concentrated suspensions of fibres in tube flow. III: Suspensions with the same fibre length distribution, Trans. Soc. Rheol., 21 (1977) 195–206.
[44] L. Nielsen, Generalised equation for the elastic moduli of composite materials, J. Appl. Phys., 41 (1970) 4626–4627.
[45] R.B. Bird, R.C. Armstrong, O. Hassager and C.F. Curtiss, Dynamics of Polymeric Liquids, Wiley, New York, Vols. 1 and 2, 1977.
[46] H. Yamakawa, Modern Theory of Polymer Solutions, Harper and Row, New York, 1971.
[47] M. Doi and S.F. Edwards, Dynamics of rod-like macromolecules in concentrated solution. Part 2, J. Chem. Soc., Faraday Trans. 2, 74 (1978) 918–932.
[48] M. Doi and S.F. Edwards, The Theory of Polymer Dynamics, Clarendon Press, Oxford, 1986.
[49] W.J. Milliken, M. Gottlieb, A.L. Graham, L.A. Mondy and R.L. Powell, The viscosity–volume fraction relation of rod-like particles by falling-ball rheometry, J. Fluid Mech., 202 (1989) 217–232.
[50] S. Haber and H. Brenner, Rheological properties of dilute suspensions of centrally symmetric particles at small shear rates, J. Colloid Interface Sci., 97 (1984) 496–514.
[51] D.H. Berry ad W.B. Russel, The rheology of dilute suspensions of slender rods in weak flows, J. Fluid Mech., 180 (1987) 475–494.
[52] S.G. Mason, Fiber motions and flocculation, TAPPI, 37 (1954) 494–501.
[53] D. Meyer and D. Wahren, On the elastic properties of three-dimensional fibre networks, Sven. Papperstidn., 67 (1964) 432–436.
[54] L.F. Carter, A Study of the Rheology of Suspensions of Rod-Shaped Particles in a Navier–Stokes Liquid, Ph.D. Dissertation, University of Michigan, Ann Arbor, MI, 1967.
[55] L.F. Carter and J.D. Goddard, A Rheological Study of Glass Fibers in a Newtonian Fluid, NASA Report No. N67-30073, June 1967.
[56] G. Christensen, Measurement of the Rheological Properties of Glass Fibre Suspensions, Dept. of Chem. Eng., Monash University, Melbourne, Vic., 1981.
[57] L.A. Faitel'son and V.P. Kovtun, Experimental study of simple shear flow of monodisperse fibrous composites, Polym. Mech., 11 (1975) 276–282.
[58] S. Goto, H. Nagazono and H. Kato, The flow behaviour of fibre suspensions in Newtonian fluids and polymer solutions. II: Capillary flow, Rheol. Acta, 25 (1986) 246–256.
[59] S. Goto, H. Nagazono and H. Kato, The flow behaviour of fibre suspensions in Newtonian fluids and polymer solutions. I: Mechanical properties, Rheol. Acta, 25 (1986) 119–129.
[60] E. Ganani and R.L. Powell, Rheological properties of rodlike particles in a Newtonian and non-Newtonian fluid, J. Rheol., 30 (1986) 995–1013.
[61] T. Kitano and T. Kataoka, The rheology of suspensions of vinylon fibres in polymer liquids. I: Suspensions in silicone oil, Rheol. Acta, 20 (1981) 390–402.
[62] R.O. Maschmeyer and C.T. Hill, Rheology of concentrated suspensions of fibres in tube flow. II: An exploratory study, Trans. Soc. Rheol., 21 (1977) 183–194.

[63] J.N. Miles, N.K. Murty and G.F. Molden, The viscosity of fibre suspensions at low fibre volume fractions, Polym. Eng. Sci., 21 (1981) 1171–1172.
[64] L.A. Mondy, T.G. Morrison, A.L. Graham and R.L. Powell, Measurements of the viscosities of suspensions of oriented rods using falling ball rheometry, Int. J. Multiphase Flow, 16 (1990) 651–662.
[65] L Nicodemo and L. Nicolais, Viscosity of concentrated fibre suspensions, Chem. Eng. J., 8 (1974) 155–156.
[66] A Attanasio, U. Bernini, P. Galloppo and G. Segre, Significance of viscosity measurements in macroscopic suspensions of elongated particles. Trans. Soc. Rheol., 16 (1972) 147–154.
[67] C.D. Han and K.-W. Lem, Rheology of unsaturated resins. I: Effects of filler and low-profile additive on the rheological behaviour of unsaturated polyester resin, J. Appl Polym. Sci., 28 (1983) 743–762.
[68] G.B. Weinberger and J.D. Goddard, Extensional flow behaviour of polymer solutions and particle suspensions in spinning motion, Int. J. Multiphase Flow, 1 (1974) 465–486.
[69] J.M Charrier and J.M. Rieger, Flow of short glass fibre-filled polymer melts, Fibre Sci. Technol. 7 (1974) 161–172.
[70] N. Malamataris and T.C. Papanastasiou, Closed-form material functions for semi-dilute fibre suspensions, J. Rheol., 35 (1991) 449–464.
[71] A. Acrivos and E.S.G. Shaqfeh, The effective thermal conductivity and elongational viscosity of a non-dilute suspension of aligned slender rods, Phys. Fluids, 31 (1988) 1841–1844
[72] E.S.G. Shaqfeh and G.H. Fredricksen, The hydrodynamic stress in a suspension of rods, Phys. Fluids A, 2 (1990) 7–24.
[73] R.A. Keiller, J.M. Rallison and J.G. Evans, Sink flows of a suspension of rigid rods: the failure of a similarity solution, J. Non-Newtonian Fluid Mech., 42 (1992) 249–266.
[74] J. Mewis and A.B. Metzner, The rheological properties of suspensions of fibres in Newtonian fluids subjected to extensional deformations, J. Fluid Mech., 62 (1974) 593–600.
[75] I.E. Kizior and F.A. Seyer, Axial stress in elongational flow of fibre suspensions, Trans. Soc. Rheol., 18 (1974) 271–285
[76] J.F.T Pittman and J. Byram, Extensional flow of polydisperse fibre suspensions in free-falling liquid jets, Int. J. Multiphase Flow, 16 (1990) 545–559.
[77] G.B. Jeffrey and A. Acrivos, The rheological properties of suspensions of rigid particles, AIChE J., 22 (1976) 417–432.
[78] K.D. Roberts and C.T. Hill, Processability/Mechanical Properties Trade-off for Reinforced Plastics, Proc. SPE Annu. Tech. Conf., 31st Pap., Montreal, Que., May 7–10, 1973, pp. 536–566.
[79] C.D. Han, Multiphase Flow in Polymer Processing, Academic Press, New York, 1981, pp. 97–98.
[80] Y. Chan, J.L. White and Y. Oyanagi, A fundamental study of the rheological properties of glass-fibre-reinforced polyethylene and polystyrene melts, J. Rheol., 33 (1978) 507–524.
[81] G.G. Lipscomb, R. Keunings, R. Marrucci and M.M. Denn, A Continuum Theory for Fibre Suspensions, in B. Mena, A. Garcia-Rejon and C. Rangel-Nafaille (Eds.), Advances in Rheology (Proc. IXth Int. Congress on Rheology), Vol. 2, Cuidad Universitaria, Mexico: UNAM, 1984, pp. 497–503.
[82] G.G. Lipscomb, Ph.D. Dissertation, University of California, Berkeley, 1986.
[83] M.C. Altan, S.G. Advani, S.I. Guceri and R.B. Pipes, On the description of the orientation state for fibre suspensions in homogeneous flows, J. Rheol., 33 (1989) 1129–1155.
[84] M. Mackay, private communication, 1993.
[85] J. Happel and H. Brenner, Low Reynolds Number Hydrodynamics, Martinus Nijhoff, The Hague, 1983.
[86] J.L. Ericksen, Anisotropic fluids, Arch. Ration. Mech. Anal., 4 (1960) 231–237
[87] D.U. Hur, Flow of Semidilute Glass Fibre Suspensions in Tubular Entry Flows, Ph.D. Thesis, Dept. Chem. Eng., University of Melbourne, 1987.
[88] G.G. Lipscomb, M.M. Denn, D.U. Hur and D.V. Boger, The flow of fibre suspensions in complex geometries, J. Non-Newtonian Fluid Mech., 26 (1988) 297–325.
[89] D.V. Boger and A.V. Rama Murthy, Normal stress difference and evaporation effects on the Weissenberg rheogoniometer, Trans. Soc. Rheol., 13 (1969) 405–408.

[90] J.G. Evans, The Effect of the Non-Newtonian Properties of a Suspension of Rod-like Particles on Flow Fields, Proc. Br. Soc. Rheol. Conf. on Theor. Rheol., 3rd Proc., Pap. and Discuss, University of Cambridge, England, 1974, John Wiley, New York, NY, 1975, pp. 224–232.

[91] M.M. Cross, A. Kaye, J.L. Stanford and R.F.T. Stepto, Rheology of Polyols and Polyol Slurries for Use in Reinforced RIM, in J.E. Kresta (Ed.), Reaction Injection Moulding, ACS Symposium Series, Washington, DC, 1985, pp. 95–110; Proc. ACS, Div. Polym. Mater. Sci. Eng., 49 (1983) 531–535.

[92] H.A. Barnes, J.F. Hutton and K. Walters, An Introduction to Rheology, Elsevier, Amsterdam, 1989.